catalysts

MDPI

Review

CeO_2-Based Heterogeneous Catalysts in Dry Reforming Methane and Steam Reforming Methane: A Short Review

Wan Nabilah Manan *, Wan Nor Roslam Wan Isahak and Zahira Yaakob *

Department of Chemical and Process Engineering, Faculty of Engineering and Built Environment, Universiti Kebangsaan Malaysia, Bangi 43600, Selangor, Malaysia; wannorroslam@ukm.edu.my

* Correspondence: p107959@siswa.ukm.edu.my (W.N.M.); zahira@ukm.edu.my (Z.Y.); Tel.: +60-12-2860347 (W.N.M.)

Abstract: Transitioning to lower carbon energy and environment sustainability requires a reduction in greenhouse gases such as carbon dioxide (CO_2) and methane (CH_4) that contribute to global warming. One of the most actively studied rare earth metal catalysts is cerium oxide (CeO_2) which produces remarkable improvements in catalysts in dry reforming methane. This paper reviews the management of CO_2 emissions and the recent advent and trends in bimetallic catalyst development utilizing CeO_2 in dry reforming methane (DRM) and steam reforming methane (SRM) from 2015 to 2021 as a way to reduce greenhouse gas emissions. This paper focus on the identification of key trends in catalyst preparation using CeO_2 and the effectiveness of the catalysts formulated.

Keywords: dry reforming methane; steam reforming methane; global warming; ceria-based catalyst

Citation: Manan, W.N.; Wan Isahak, W.N.R.; Yaakob, Z. CeO_2-Based Heterogeneous Catalysts in Dry Reforming Methane and Steam Reforming Methane: A Short Review. *Catalysts* **2022**, *12*, 452. https://doi.org/10.3390/catal12050452

Academic Editors: Gang Feng, Supawadee Namuangruk and Yan Jiao

Received: 31 December 2021
Accepted: 2 February 2022
Published: 19 April 2022

1. Introduction

In the 21st century, global warming and climate change are widespread issues that plague our planet due to the increase in greenhouse gas (GHGs) emissions. Carbon dioxide (CO_2) and methane (CH_4) are the most plenteous greenhouse gases that contribute to today's climate change issues which have brought catastrophic changes to the global weather [1]. These issues are related to the burning of fossil fuels including oil, coal and gas to meet the demands of energy consumption which are driven by population and economic growth [2]. The world is now shifting to lower carbon energy to combat this issue. Governments and private sectors around the globe are making collective efforts to reduce emissions of greenhouse gases.

Six years have passed since the Paris Agreement target which was signed in December 2015 by 195 countries to fight climate change [3]. The goal of the Paris Agreement was to contain the rise of the global average temperature at well below 2 °C above pre-industrial levels and to limit the temperature increase even further to 1.5 °C by 2100 [4]. Recently, many oil and gas global companies such as Shell, BP and Petronas have stated they are moving towards net zero carbon emissions by 2050 [5–7]. The EU, Japan and South Korea, together with more than 110 countries, have vowed to obtain carbon neutrality by 2050 while China says it will do so before 2060 [8]. This change is one of the consequences of the Paris Agreement's ratification.

When the COVID-19 pandemic hit the world in 2020 and 2021, the world experienced a record decline in global CO_2 emissions due to the unprecedented cessation of human activities. The decreases in industry resulted in decreases in emissions (157.9 Mt CO_2, 7.1% compared to 2019), followed by road transportation (145.7 Mt CO_2, −8.3%) and power generation (131.6 Mt CO_2, −3.8%) [9]. Recently, in September 2021, the world lockdown measures were lifted and energy demand is expected to continue growing which will undoubtedly increase greenhouse gas emissions.

In this paper, we will discuss a method of CO_2 emission management, the methane reforming process, which focuses on dry reforming and steam reforming and utilizes

CeO_2 as a rare earth catalyst. The paper will also focus on the advancements made from 2015 to 2021. Our analysis focuses on the identification of key trends in catalyst preparation using cerium oxide (CeO_2) and the effectiveness of the catalyst formulated.

1.1. CO_2 Emission Management

CO_2 is a stable gas with a bond strength of 532 kJ mol^{-1} and is the key molecule in global warming [10,11]. Anthropogenic human activities are the cause of fossil fuel dependency and cement production. Industry emissions from fossil fuels and the combustion of steel, chemicals and other manufactured products as well as cement production process on average 29% of the global CO_2 emissions [12]. The anthropogenic CO_2 emissions from fossil fuel consumption have caused the CO_2 concentrations in the past 50 years to continually rise [13,14]. The detrimental effects of climate change on the environment are endangering our lives as they entail myriad problems such as air pollution, water contaminations, land degradation and flash floods. Climate changes are occurring more rapidly nowadays which has resulted in an increase in many extreme weather events including heatwaves and extreme bushfire conditions [15].

This climate crisis urgently calls for a renewable energy shift and the conversion of CO_2 into fuels is seen as strategic part of CO_2 emission management. Since CO_2 is a natural source of carbon [16], it can be catalytically converted via several routes to generate useful fuels and chemicals [17,18]. Nevertheless, there are still chemical and technological obstacles in the utilization of CO_2 as the C1 building block due to its inert nature and very high energy bond [19]. Carbon dioxide capture and storage (CCS) was introduced to minimize carbon dioxide emissions by capturing and storing CO_2 in enormous quantities [20]. The technologies related to the capture and separation of CO_2 offer great industrial opportunities and advantages [21]. On the other hand, carbon capture and utilization (CCU) is targeted at generating value by exploiting CO_2 as a raw material [22]. Utilizing CO_2 as a chemical feedstock produces organic chemicals in a safer way as opposed to the toxic phosgene in the organic synthesis of polycarbonates and allows for the production of new chemicals with zero cost. These CCU technologies can create a positive reputation for companies due to the political and social pressures related to global warming [23].

1.2. Methane Reforming

Methane, which has a bond strength of 434 kJ mol^{-1}, [24] is produced naturally from sources such as termites, grasslands, wildfires, lakes, and wetlands and is also produced from human activities such as coal mining, landfills, oil and gas processing and agricultural activities [1,22]. Methane, which constitutes natural gas, has been identified as the second most dangerous and abundant greenhouse gas that is emitted [23]. Methane can be used directly for heat and electricity production as well as for the production of syngas via the reforming process [24]. Methane can be reformed through three routes, namely steam reforming methane (SRM), dry reforming methane (DRM) and the partial oxidation of methane (POM) [25]. In all routes, the processes use an oxidizing agent that oxidizes methane to carbon monoxide whilst producing hydrogen in a ratio that will vary depending on the type of oxide used [24].

Steam reforming methane (SRM) is the oldest and most widely practiced production route for syngas [26,27]. It is the outcome of the reforming (Equation (1)) and the Water Gas Shift (WGS) reactions (Equation (2)).

$$\text{SRM: } CH_4 + H_2O \leftrightarrow CO + 3H_2 \ (\Delta H298K = +206 \text{ kJ mol}^{-1}) \quad (1)$$

$$\text{WGS: } CO + H_2O \leftrightarrow CO_2 + H_2 \ (\Delta H298K = -41 \text{ kJ mol}^{-1}) \quad (2)$$

However, this process requires high temperatures (typically above 800–900 °C) and a large amount of steam to proceed [28].

Dry reforming methane (DRM) is acknowledged as an alternative for steam reforming (SRM) because it can directly utilize raw natural gas and does not require subsequent gas separation and purification to remove CO_2 [29].

Dry reforming methane (DRM) has been in the spotlight as this reaction has the advantage of solving two issues related to the reduction in greenhouse gas (GHG) emissions since it uses (CH_4 and CO_2) as feed stocks to produce valuable syngas (CO and H_2). Over the years, dry reforming of methane has been investigated critically and extensively by many scientists [25,30–36]. Syngas is an important precursor for the production of high-chained hydrocarbon fuels and value-added oxygenated compounds [37]. DRM yields the H2 to CO unit ratio (1:1) needed for Fischer–Tropsch synthesis [32]. This unit ratio is desirable for many gas to liquid (GTL) applications. Apparently, the indirect routes of methane conversion to liquid fuels (via syngas) are more efficient than direct conversion and are the most widely used routes in the GTL industry [38].

$$CH_4 + CO_2 \leftrightarrow 2CO + 2H_2 \ (\Delta H298K = +247 \text{ kJ mol}^{-1}) \quad (3)$$

Coke depositions are unavoidable in DRM reactions as the deposits will be generated from two side reactions, namely the Boudard reaction (3) and methane cracking (4):

$$2CO \rightarrow C + CO_2 \ (\Delta H298K = -172 \text{ kJ mol}^{-1}) \quad (4)$$

$$CH_4 \rightarrow C + 2H_2 \ (\Delta H298K = +75 \text{ kJ mol}^{-1}) \quad (5)$$

DRM is seen as a high potential process technology in the current fluctuating low oil price regime due to its higher CO selectivity and low H_2/CO ratio, which are suitable for the synthesis of long chain hydrocarbons or oxygenated chemicals such as acetic acid, dimethyl ether and oxo-alcohols [4].

The further conversion of syngas is very important for chemical industries that produce commodity goods for human lives and comfort which are essential in agriculture, hygiene, health, food science, pharmaceuticals, construction, vehicles and petrochemicals.

1.3. The General Strategy for Formulating the Catalyst

The development of catalysts is a critical component of the ongoing search for novel methods of enhancing the yield and selectivity of chemical reactions. A catalyst makes it possible to obtain an end product by different pathways with lower energy barriers [39]. Previously, noble metals (e.g., Rh, Pt, Pd and Ru) and base metals such (e.g., Iron, Nickel and Zinc) were studied as catalysts for DRM reactions [40]. Noble metals have a superior capability to break the C-H bond and suppress carbon deposition [41]. However, due to the high costs of noble metals, Nickel-based catalysts are more preferable in the DRM process as they are cheap, abundant and demonstrate a high catalytic activity and availability. Nevertheless, Nickel-based catalysts have weaknesses in terms of their proneness to sintering and coking at high temperatures [42,43].

The main driving force for DRM reactions is the presence of active sites for the dissociation of CH_4 and CO_2. Bifunctional active sites utilize both loaded metals and supports as sites for reactant activation [42]. There is evidence that the presence of a base metal in the catalysts can suppress the formation of coke during the decomposition of CH_4 and the Boudard reaction [44]. The basicity of a catalyst contributes to its activity by facilitating the chemisorption, activation and decomposition of acidic CO_2 gas in the presence of an active metal phase. This increases the surface coverage of CO_2 on the catalyst, reduces the carbon deposition from the Boudard reaction and lowers the reactant activation barrier [42].

Nanocrystals, which are only a few nanometers in size, present the best catalytic efficiencies. As explained by Vedrine [45], nanoscience has encouraged bottom-up strategies. The performance of a solid catalyst relies on its grain size, shape, composition and preparation. Usman et al. [46] agreed that the preparation methods play an important role

in the synthesis of smaller particle sizes and in the higher dispersion of the active metal. Metal particles produced in the small size range (1–10 nm) experiences difficulties related to their application in the reactor; therefore, support bodies are required. Supports play a key role in the enhancement of catalytic activity and the suppression of carbon deposition in dry reforming methane [31].

For decades, various catalyst configurations, morphologies and topologies have been tested to determine how synergistic component interactions influence active metal dispersion, basicity, redox property, oxygen mobility, particle size, size distribution, reducibility and the mass transfer limitations of catalysts [42,47]. The most common strategy is to include the application of supports and promoters with a high basicity in order to increase the CO_2 adsorption capacity, as well as to improve the oxidation of carbonaceous species via the Boudard reaction. Another approach is to increase the interactions between the active phase of the nickel and support and thus inhibit sintering [48].

2. Ceria

Cerium (Ce) is a versatile and important rare earth element that has been involved in many areas of heterogeneous catalysis for several years [49–52]. It is the most reactive element of the lanthanide series with reserves that are much higher than copper and tin (66.5 and 60 ppm, respectively) [53]. As shown in Figure 1, it has a fluorite structure (FCC) with a space group Fm3m and it consists of a simple cubic oxygen sub-lattice with cerium ions occupying alternate cubes [53,54]. Each Ce cation is surrounded by eight oxygen atoms and the coordination number of the oxygen atoms is four [55]. CeO_2 contains an oxygen deficient (CeO_{2-x}, with $(0 < x \leq 0.5)$ in a reducing condition which is considered as a partially reduced oxide. This property facilitates readily oxidized to CeO_2 by capturing oxygen in an oxidizing condition [56,57].

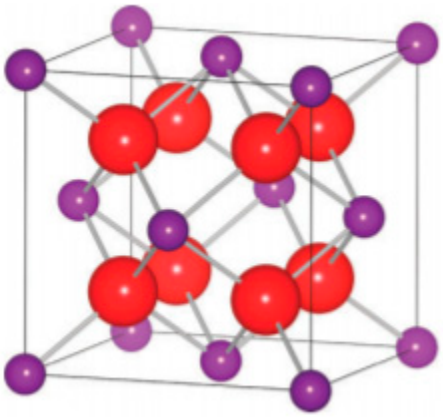

Figure 1. The FCC structure of cerium oxide (CeO_2). Reprinted with permission from [54], copyright Elsevier, 2010.

There are many factors that explain why CeO_2 rare-earth oxides have dominated in technological applications in the field of catalysts [58]. The reasons include their environmental friendliness, surface-bound defects, excellent redox ability and remarkable oxygen storage capacity and release ability. They have strengths such as the ability to stabilize metal dispersion and promote the water–gas shift [59,60]. CeO_2 can be used as an oxygen reduction reaction (ORR) catalyst due to its ability to switch between Ce^{4+} and Ce^{3+} oxidation states which leads to decent ionic conductivity and good oxygen sorption [55,61]. The presence of oxygen vacancies on the surface often dramatically alters the adsorption and subsequent reactions of various adsorbates, either on a clean surface or on metal particles supported on the surface [62]. The modification oxidation state of the metal catalyst cab influence the absorption behavior of the reactants and the subsequent conversion of the reaction intermediates and the reaction path. Therefore, CeO_2 is a highly tunable material with great potential for CO_2 catalysis due to its unique properties [63].

CeO_2 recorded its first appearance in 1979 when it was observed to have the ability to promote dispersion in comparison with conventional supports such as Al_2O_3 [64]. Since the first discovery, it has been identified in various roles such as promoting noble metal dispersion, promoting the water–gas shift (WGS) and the steam reforming reactions, favoring catalytic activity at the interfacial metal–support sites, promoting CO removal through oxidation by employing a lattice oxygen as well as storing and releasing oxygen (oxygen storage capacity, OSC) under lean and rich conditions, respectively in three-way catalysts (TWCs) [64].

2.1. Ceria as a Support

Supports play important roles in the dispersion, activity and stability of active sites. The role of a support is to provide a high surface area for the dispersion of metals, to give resistance to sintering and to stabilize and promote active sites. They may participate in the reaction itself and can modify the catalytic properties of the active phase and increase resistance to coking [11,65]. The support also plays an active role in the catalytic reaction. It provides certain physiochemical properties such as basicity (CaO, La_2O_3 and MgO), oxygen storage capacity (CeO_2, CeO_2-ZrO_2 and TiO_2) and reducibility (CeO_2 and ZrO_2) [4]. Acidic supports directly affect the mechanism which favors carbon deposition while basic supports facilitate good effects such as high affinity for CO_2 chemisorption and oxygen mobility [66].

CeO_2 is a good support for a noble metal catalyst and ensures long-term use due to its unique properties that have been mentioned (strong metal support, OSC, reducibility (Ce^{4+}/Ce^{3+}) and soot resistance. These properties of CeO_2 enhance the ability of noble metals in a reaction compared to a support with an inert nature such as Al_2O_3, especially for SRM, DRM and WGS reactions [67]. Generally, a high surface area provides a greater tendency for active species to make contact with reactants; therefore, they enhance catalytic performance [53].

Luisetto et al. [65] explained that the oxygen vacancies on the CeO_2 surface may adsorb the oxygen formed by the dissociation of CO_2, improving the reforming activity and the removal of carbon deposits. CeO_2-Al_2O_3 combinations are excellent supports for reforming reactions due to their lower acidity in comparison to bare alumina and the greater oxygen capacity storage (OCS) of CeO_2. Adding CeO_2 to form a CeO_2-Al_2O_3 support improves reducibility and enhances the oxygen mobility and metal dispersion [68]. The redox properties of ceria facilitate the oxidation of carbon deposits which expand the lifetime of the catalyst [69]. CeO_2 can modify the metal–support interactions of the Ni catalyst, which can improve the reducibility of the Ni/Al_2O_3 catalyst [70]. Several studies have revealed that ceria modifies metal–support interactions, increasing the active phase dispersion and improving the stability of alumina at high temperatures [71].

Farooqi et al. [72] made a comparison of three synthesis catalysts namely Ni/Al_2O_3, Ni/Al_2O_3-CeO_2 and Ni/Al_2O_3-La_2O_3. It was discovered that the addition of CeO_2 as a combined support with Al_2O_3 improved the dispersion, increased the active metal content on the catalyst surface and enhanced the reducibility and the catalyst basicity. Similar findings by Chein [73] revealed that high carbon-resistant Ni/Al_2O_3 with a CeO_2-modified catalyst was produced due to the fact that the $CeAlO_3$ phase suppressed coke formation without damaging the catalytic activity, inhibited the growth of graphitic carbon, decomposed CO_2 and formed active surface oxygen.

Huang et al. [74] indicated that adding CeO_2 to a Ni/Mo/SBA-15 catalyst used for DRM was beneficial. Catalysts with low CeO_2 amounts (up to 2 wt%) showed more stability than Ni/Mo/SBA-15 during dry reforming methane. The addition of CeO_2 helped small metallic Ni particles to be stably dispersed on the composite support and also enhanced the reducibility of the catalysts and adsorption of CO_2 during the reaction. Huang et al. [74] also stated that CeO_2 actually has dual roles in preventing carbon deposition in the CO_2 reforming of methane. The addition of CeO_2 decreased the acidity of the support. This

stopped the formation of pyrolytic carbon and the basic CeO_2 helped the chemisorption and dissociation of CO_2 and subsequently accelerated carbon elimination.

Strong metal–support interactions and abundant oxygen vacancies are very important to prevent the sintering of nickel particles as depicted in research by Xianjun et al. [75]. As shown in Figure 2, methane first absorbs on the active Ni particles and then decomposes into CHx, while carbon dioxide absorbs Ni particles and decomposes into carbon monoxide and O *. Active intermediates containing CHx and O * can react with each other to produce carbon monoxide and hydrogen. Lattice oxygen replenishment results from CO_2 dissociation and oxygen mobility.

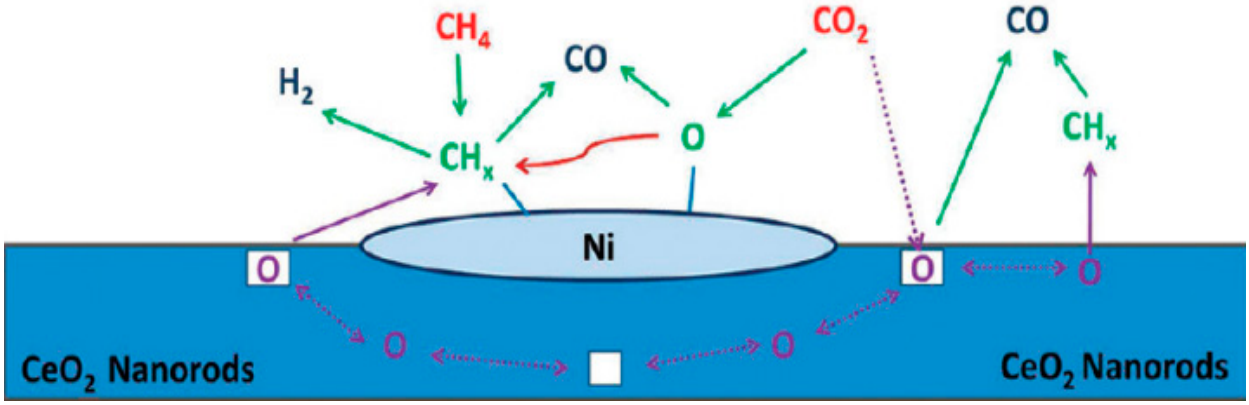

Figure 2. Catalytic mechanism diagram for DRM over Ni-supported ceria nanorods. Reprinted with permission from [75], copyright ACS, 2012.

Supports can influence the chemical state of noble metal nanoparticles other than simply acting as a substrate for the dispersion of the loaded metal. Controlling the size and uniformity of a supported metal catalyst is a major challenge for the catalytic structure–property relationship. To generate monodisperse metal catalysts, molding agents or surfactants with a significant adhesion for the metal surface are typically used, masking the catalyst's intrinsic catalytic behavior [76].

2.2. Ceria as a Promoter

The function of chemical promoters is to present new, supplementary active sites or to reinforce the chemical property relating to the reactivity of the catalyst such as basicity and redox properties [4]. The addition of promoters can aid in the reduction in carbon deposition and sintering, as well as the oxidation of carbonaceous species, resulting in an improved reaction conversion.

The addition of CeO_2 into catalysts demonstrates the positive effects on catalytic activity and stability and carbon suppression when it is used as a promoter instead of a support with a strong metal–support interaction, which reduces Ni sintering and carbon deposition [74]. The work by Li et al. [77] found that adding 3 wt% of Ce could suppress the sintering of Ni particles on SBA-15 by promoting the oxidation of coke formed on the nickel catalyst based on its internal oxygen transfer to coke. Applying a Ce promoter has its own advantages. Ce doping inhibits reactions (3), increases the catalyst basicity and CO_2 adsorption and favors the oxidation of deposited carbon species [48].

Arora and Prasad [32] stated that promoters such as Sn, Sr, Ca, Ce, K and Zr are employed to prevent carbon accumulation and the combination of Ce, Zr and transition metals has garnered interest due to their oxygen storage abilities. They give an oxygen lattice in the Ce oxide phase during reducing conditions and generate anionic vacancies which enhance the activity of the catalyst.

Adding promoters (e.g., Co, ZrO_2, CeO_2, MgO and CaO) to a nickel-based catalyst is an effective way to promote Ni/Al_2O_3. CeO_2 can modify the metal–support interaction of Ni catalysts, which can improve the reducibility of the Ni/Al_2O_3 catalyst [78].

Mallikarjun et al. [79] suggested that the promotion of alkali metals can enhance the carbon resistance in a Ni-based catalyst. The higher activities of catalysts modified with Ce and CO_2 can be explained on the basis of the $CeAlO_3$ formed, which interacts with Ni differently when compared to CeO_2 and Al_2O_3 alone. The highest catalytic activity was attributed to the formation of an interface between Ni and Ce, which acted as an active site for methane activation [46].

Many researchers have reported on the use of bimetallic systems, as doping with other metals can improve catalytic performance in the DRM reaction [80,81]. The doping of a second metal can enhance the adsorption properties of CO_2 and H_2O which is beneficial for reactions with carbon and for reducing carbon deposition [81].

3. Summary of DRM with CeO_2-Based Catalysts from 2015 to 2021

Ay et al. [82] found that the Co/CeO_2 catalyst exhibited a much lower performance than the Ni/CeO_2 and $Ni\text{-}Co/CeO_2$ catalysts due to strong metal–support interactions. The activities of ceria-based catalysts decreased with an increase in the calcination temperature accompanied by a decrease in coke deposition.

T. Stroud et al. [83] highlighted that through the addition of small quantities of dopants such as Sn and CeO_2, the DRM performance can be improved. As shown in Figure 3, the optimum amount of the Ni/Sn molar ratio was identified to be 0.02. This multicomponent catalyst, Sn0.02Ni/Ce-Al, remains active for long periods of 92 h with 85% CO_2 conversion. Sn atoms were found occupying C nucleation sites in the vicinity of Ni atoms which slowed down the carbon formation, whereas the presence of ceria provided a high oxygen storage capacity and modified the acid/base properties of the support lead with alumina.

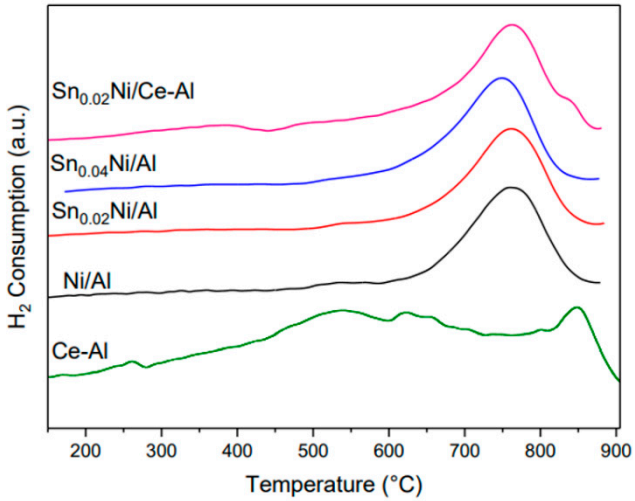

Figure 3. H_2-TPR profiles of each catalyst. Reprinted with permission from [83]. Copyright Elsevier, 2017.

Mallikarjun et al. [79] developed Ni/CeO_2-SrO by the impregnation method and pronounced that the catalyst with 12wt% Ni and equal mole ratios of CeO_2-SrO showed better activity and showed extraordinary stability over a period of 250 h. The Ni dispersion and metal reducibility were improved by the addition of CeO_2.

Akiki et al. [84] revealed that a catalyst based on 5 wt% of Ni can be used as an optimal concentration for DRM and the effect of Ce is more beneficial than La as a promoter. The $1.5Ce\text{-}Ni5/MgAl_2O_4$ catalyst exhibited the best catalytic activity and stability for DRM with 96% CO_2 conversion and 92% CH_4 conversion. Strong interactions between the CeO_2 and the support enhanced the structure of the catalyst, resulting in the creation of more oxygen vacancies.

Jin et al. [85] deposited Ni nanoparticles on the four channels of the α-Al_2O_3 hollow fibers catalyst support by using atomic layer disposition (ALD). The $CeNi/Al_2O_3NP$ catalyst was prepared by the incipient wetness (IW) method and was stable for 360 h which

was 7.5 times longer than Ni/Al_2O_3NP-ALD and produced an excellent performance after regeneration. The higher stability for the Ni-based catalyst was achieved due to the strong oxygen storage and release properties of CeO_2 which improved the CO_2 dissociative adsorption reaction and lead to reduced carbon formation.

Jawad et al. [68] investigated a series of Ni-based Al_2O_3-CeO_2 composite catalysts which showed a significant improvement with the addition and doping of third metal particles such as Pt, Fe and Mo within the bimetallic catalyst due to enhanced metal dispersion and catalyst reducibility. The Ce and MOx-modified catalysts demonstrated increased redox properties and abundant oxygen vacancies among the Ni-based composite catalysts which provided supplement active oxygen and more active sites for the activation of CO_2 and CH_4.

Karemore et al. [86] studied the influence of reaction conditions (temperature, space time, feed composition and time-on-stream) and reaction kinetics on a mixed reforming methane reaction using Ni-K/CeO_2-Al_2O_3 to facilitate catalyst development and a reactor design for the reaction. The reactant conversion and product yield increased with the increase in space, time and temperature. The presence of the promoters K and CeO_2 oxidized the carbon formed on the catalyst surface and caused the carbon deposition rate over 50 h to be low (2.45 mgC/gcat-h). The syngas (H_2/CO) ratio at 800 °C significantly increased from 1.32 to 2.14 mol/mol with the increase in the S/C ratio of 0.2–0.5 mol/mol.

Chein et al. [73] studied the reactant composition to determine the performance and stability of the catalyst using a modified Ni/Al_2O_3 catalyst. The carbon resistance increased on the catalyst's surface with the modification of CeO_2 on the Ni catalyst and the addition of O_2. As the number of CeO_2 loading increased, the CH_4 conversion increased. However, as shown in Figure 4, the CH_4 conversion obtained from 10Ni15Ce catalyst was lower than that from the 10Ni10Ce and 10Ni5Ce catalysts. The conversion of 10Ni15Ce was almost the same with 10Ni0Ce. Hence, it was concluded that the optimum amount of CeO_2 loading was in the range of 5 to 10% for the best DRM performance due to the decrease in the specific surface area as the CeO_2 loading increased and the Ni particle aggregation increased. The addition of O_2 significantly suppresses the RWGS reaction in DRM due to the dominance of the CH_4 oxidation reaction. These findings concur with the research by Arora and Prasad [32] which stated that the addition of oxygen to SRM and DRM can improve the energy efficiency or synergistic effects in the processing and mitigation of coking.

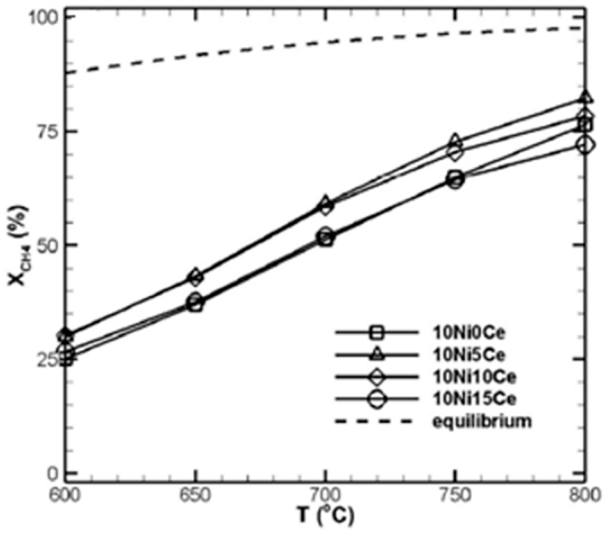

Figure 4. CH_4 conversion obtained from the 10Ni15Ce catalyst is lower than that from the 10Ni10Ce and 10Ni5Ce catalysts. Figure republished with permission from [73]. Copyright Elsevier, 2019.

Swirk et al. [87] studied DRM double-layered hydroxides modified with cerium (co-precipitation method) and with yttrium prepared by the incipient wetness impregnation method with 0.2, 0.4 and 0.6 wt%. Ni reducibility decreased, basicity increased, Ni dispersion enhanced and smaller Ni crystallites were observed with the promotion of both Ce and Y, as compared with a hydrotalcites catalyst due to the formation of a yttria-doped ceria (YDC) phase. Highlighted in the studies was the modification of the smallest loading of yttrium (0.2 wt%) which led to an increase in both CO_2 and CH_4 conversions for 5 h.

Zhang et al. [88] investigated the effect of adding Zr dopants into the ceria support, $Ni/CeZrO_2$, on the DRM reaction performance and revealed that the conversion, reaction rate and H_2 selectivity substantially increased with the addition of a Zr dopant. A larger Ce^{3+} substance was noticed in the mixed-oxide support upon the reaction with pure CH_4 or during DRM, when doping the Zr into the ceria support implied a higher reducibility of the mixed-oxide support. Moreover, Zr prevented Ni migration from the surface into ceria forming a $Ce_{1-x}Ni_xO_{2-y}$ solid solution which maintained the active NiO on the $Ni/CeZrO_2$ surface.

Hassani Rad SJ, et al. [89] prepared Ni/Al_2O_3-CeO_2 and Ni/Al_2O_3-MgO nanocatalysts using the impregnation and sol-gel methods. The sol-gel method produced a better performance compared to the impregnation method as it provides a much higher surface area, a better dispersion of metals, a more homogenous morphology and a smaller nanoparticle size leading to modified adsorption properties. Among all, the sol-gel method synthesized with the ceria promoter catalyst and the Ni/Al_2O_3-CeO_2 nanocatalyst emerged as the best choice as it exhibited a H2/CO ratio of 1 and a H2 yield of 94% at 850 °C.

Farooqi [72] compared the performances of three catalysts, namely Ni/Al_2O_3, Ni/Al_2O_3-CeO_2 and Ni/Al_2O_3-La_2O_3 which were prepared by the sol-gel method. The catalyst with the addition of CeO_2 on the support showed the highest and most stable conversion due to the fact that it enhanced dispersion, increased the active metal content on the catalyst surface and improved the reducibility and basicity of the catalyst.

Price et al. [90] highlighted that encapsulation techniques with incorporations of 8 wt% Ni/ZnO cores in silica (SiO_2) can lead to advantageous conversions of CO_2 and CH_4 at high temperatures compared to uncoated traditional catalytic materials: Ni/CeO_2 and Ni/Al_2O_3. Encapsulating a catalytic core increases the surface area and reaction kinetics which results in a high level of reactant conversion.

Das et al. [91] developed a novel core-shell structured Ni-SiO_2@ CeO_2 catalyst with Ni nanoparticles sandwiched between SiO_2 and CeO_2 layers as shown in Figure 5, applied for the dry reforming of bio-gas (CH_4/CO_2 = 1.5) at low temperatures (600 °C). Ni-SiO_2@CeO_2 produced a higher Ni dispersion which resulted in a superior performance compared to its bare structure with negligible coke formation during a 72-h stability test and high dry reforming activity (~0.12 mol CH_4 $min^{-1}gNi^{-1}$). The dual confinement effect provided by the encapsulation of Ni nanoparticles between SiO_2 and CeO_2 layers prevents Ni sintering and the redox capacity of CeO_2 and the higher RWGS activity of ceria leads to a high coke resistance for the catalysts.

K. Han et al. [92] synthesized Ni@SiO_2@CeO_2 by coating ceria on the surface of Ni@SiO_2 which was initially prepared by the reverse microemulsion method. Ni@SiO_2@CeO_2 exhibited a bi-functional mechanism compared to the mono-functional mechanism of Ni@SiO_2 which resulted in a one and a half times higher catalytic performance and a reduced carbon deposition at low temperatures of 400 to 600 °C which indicated high stability.

Cardenas-Arenas et al. [93] demonstrated that nanoparticle catalysts, designated NiO-CeO_2, synthesized by the reversed microemulsion process were capable of lowering 63% of carbon deposition during the DRM test. Triton X-100, n-heptane and hexanol were used to create the microemulsion. The nanoparticles' small size facilitates the participation of cerium cations in the redox reactions that occur during DRM and stabilizes the nickel cationic species.

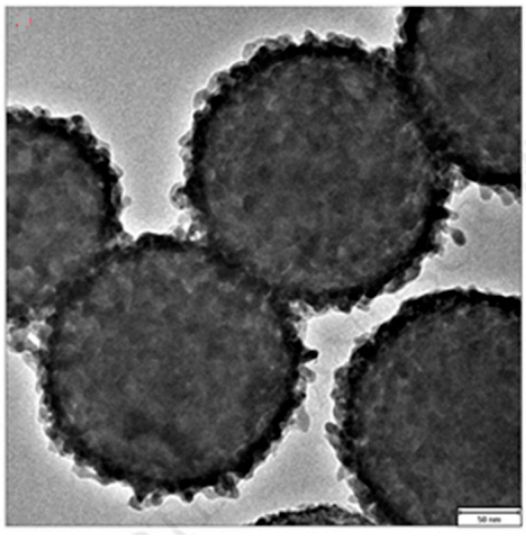

Figure 5. TEM image for reduced Ni-SiO_2@CeO_2. Figure republished with permission from [91] Copyright Elsevier, 2018.

Marinho et al. [94] highlighted that the Ni catalyst synthesized by the EISA method produces materials with a high surface area and well defined mesopores. It favors the formation of the $NiAl_2O_4$ spinel phase with very well dispersed Ni particles on the support and inhibits sintering at high temperatures. The addition of cerium promotes oxygen mobility when interacting strongly with Al_2O_3 and enhances the carbon resistance and catalytic performance.

Luisetto et al. [65] synthesized a Ni catalyst supported by a solid solution of CeO_2 with Zr, Sm and La dopands using the one-step citric acid method. The most promising catalysts in terms of low carbon formation were Ni/Sm-DC and Ni/La-DC, as the nature of the dopants influenced the Ni–support interaction and the electronic state of the metal catalyst.

Padi et al. [95] suggested that the exsolution process in the nanoscale NiO-CeO_2 solid solution with a fluorite structure could produce the supported Ni/CeO_2 catalyst. In Figure 6, the elemental mapping by STEM-EDX highlights the grain boundaries and stacking faults after 90 h of the DRM reaction which provides nucleation sites for nanoparticle growth. This Ni/CeO_2 catalyst demonstrated an active and stable performance in DRM at 800 °C for 50 h which verified the strong metal–support interaction with no coking at all. The outstanding result was due to the combination effect of the strong metal–support interaction derived by the exsolution method and the existence of a highly mobile oxygen lattice within the ceria support. Coking on a CeO_2-supported material can be prevented without the need to add a second oxide to the final support phase. The composition of catalyst supports attributable to the effects of size and charge balance is noted in this method.

Zhang Q et al. [96] introduced a novel photoactivation using UV-Visible Infrared (UV-Vis-IR) illumination to improve the solar-light-driven thermocatalytic activity of a Ni/CeO_2 catalyst in DRM. The synergetic effect among the Ni nanoparticles and CeO_2 exists for DRM on the catalyst derived from the migration of the oxygen lattice at the Ni–CeO_2 interface. The improved catalytic activity of the Ni metal was confirmed by the DFT calculation in which the irradiation reduces the activation energy of the dominant steps of C and CH oxidation.

Using a plasma decomposition method, X. Yan et al. [70] synthesized two types of catalysts with distinct interfacial structures and interactions between Ni and CeO_2. The first catalyst, designated Ni/CeO_2-SiO_2-P, included CeO_2 with a higher concentration of reactive oxygen species in close proximity to Ni NP, whereas the second catalyst, designated Ni/CeO_2-SiO_2-C, contained CeO_2 that was separated from Ni NP. The Ni/CeO_2-SiO_2-P

catalyst outperformed the Ni/CeO_2-SiO_2-C catalyst in terms of performance and stability in DRM. The superior performance of Ni/CeO_2-SiO_2-P is due to the unique interface structure, which promotes the formation of formate species and the reaction of original and active Cα species via more available oxygen species and more accessible hydrogen sites on the metal–support interface, whereas in Ni/CeO_2-SiO_2-C, the insufficient conversion of Cα results in the accumulation of less active Cβ species and Cγ, deactivating the catalytic performance.

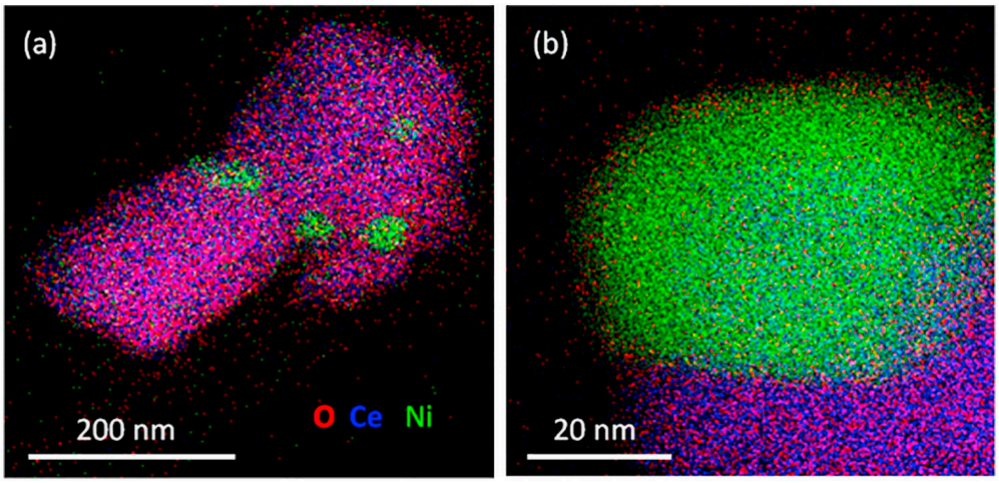

Figure 6. (**a**) low and (**b**) high magnification STEM-EDX elemental display of Ni/CeO_2 exsolved from $Ce_{0.97}Ni_{0.33}O_2$-δ after 90 h of DRM at 800 °C. Figure republished with permission from [95]. Copyright Elsevier, 2020.

Tu PH et al. [97] invented a new two-step hydrothermal process which produced flowerlike $Ce_{0.5}Zr_{0.5}O_2$ with an OSC of 536 $\mu molO_2 g^{-1}$ which was double the OSCs of pure flowerlike CeO_2 (284 $\mu molO_2 g^{-1}$). The function of ceria (CeO_2) as a support material for the Ni catalyst in DRM was improved by producing a solid solution (SS) with zirconia (ZrO_2) to raise the OSC. The flowerlike $Ce_{0.5}Zr_{0.5}O_2$ synthesized by a two-step hydrothermal process as shown in Figure 7 produced the highest catalytic performance for DRM at 750 °C with an initial methane conversion of 88.4% compared with the $Ce_{0.5}Zr_{0.5}O_2$ synthesized by the one-step hydrothermal process with methane conversion of 83.7%. The author concluded that the petals of the flowerlike structure elevated the sintering resistance of the Ni metal and the coking resistance due to a high OSC.

Simonov et al. [98] prepared mixed ceria-zirconia oxides including those doped by Nb and Ti by the traditional citrate method and by continuous solvothermal flow synthesis in supercritical alcohols. It was observed that the catalyst prepared in supercritical alcohols was the most active and stable from the rest with the specific activity doubling after the addition of Nb and Ti due to the strengthening of the metal–support interaction and the increase in OSC.

Fedorova et al. [99] investigated the effect of Ni loading methods prepared by incipient wetness impregnation and the one-pot technique on the catalytic behavior of DRM. The results established that the catalytic activity is dependent on the composition of the support and the method of Ni deposition. The effective activation energy of DRM over the impregnated sample was demonstrated to be lower than that of the one-pot series. The TOF increased three times when titanium and niobium cations were added to nickel-containing catalysts based on ceria-zirconia. The author found that the "one-pot" method in a supercritical medium for the preparation of catalysts is advantageous due to its pace of production and scalability.

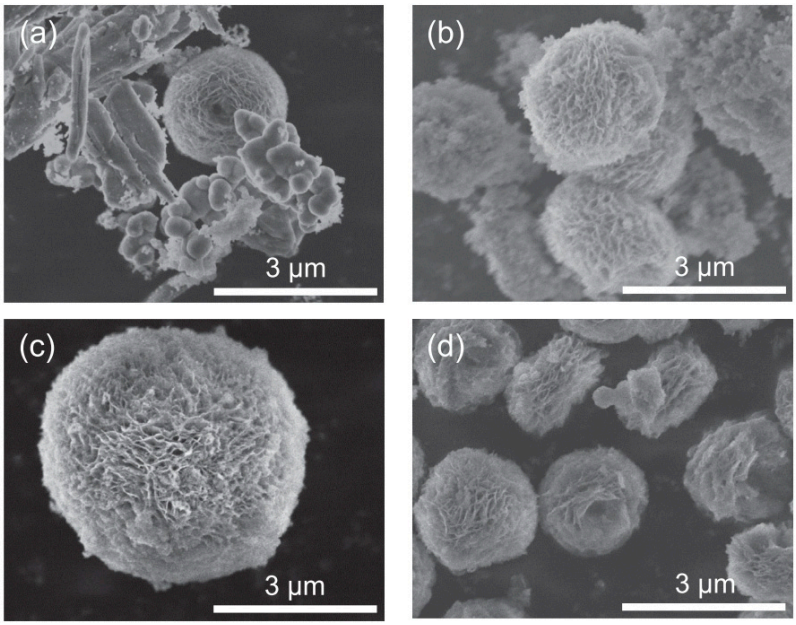

Figure 7. FESEM images of flowerlike CeO_2-ZrO_2 developed using a two-step hydrothermal process: (**a**) CZ(2Hyd0.5a) and (**b**) CZ(2Hyd0.5b). (**c**,**d**) are the $Ce(OH)CO_3$ precursors after 72 and 48 hours, respectively, of the initial hydrothermal process (1st step). Figure republished with permission from [97]. Copyright Elsevier, 2021.

Bin Li et al. [100] prepared porous silica-supported nickel catalysts (Ni-CeX-Y/SiO_2) with different contents of CeO_2 by the "one-pot" method and discovered that the addition of CeO_2 hindered the formation of the 1:1 Ni-phyllosilicate species and weakened the interaction between Ni and Si but could efficiently prevent the sintering of Ni nanoparticles and therefore Ni-CeX-Y/SiO_2 catalysts possess excellent anti-sintering ability. Moreover, the kinetic study revealed that the introduction of CeO_2 is this method could decrease the activation energy of CH_4 decomposition and CO_2 dissociation. The active oxygen species from CeO_2 and the increasing number of O* derived from CO_2 dissociation resulted in the decrease in carbon deposition in CH_4 decomposition which verified that the useful effect on the gasification rate was more powerful than the rate of carbon formation. Hence, the stability of the Ni-CeX-Y/SiO_2 catalyst improved exceptionally by increasing CeO_2 loading.

Jeon et al. [101] observed that when CeO_2 was added to a Ni-MgO catalyst constructed at various titration rates, the OSC effect changed and had an effect on not only the catalytic activity, but also the stability. Without adding CeO_2, the influence of the titration rate on Ni-MgO catalysts is limited to changes in Ni crystallite size and dispersion, which are capable of altering the catalytic activity during DRM. Thus, the Ni-MgO-CeO_2 catalyst synthesized at a rapid titration rate demonstrated the greatest DRM performance at 800 °C and a high gas hourly space velocity of 720,000 $mL \cdot g^{-1} \cdot L^{-1}$.

Lustemberg et al. [102] elucidated the nature of the active sites in Ni/CeO_2 catalysts for DRM and direct methane to methanol conversion. Due to the discovery that Ni at low loadings on CeO_2 (111) is particularly active in DRM, Lustemberg and coworkers correlated experimental observations on the CeO_2 (111) surface with clusters of tiny cationic Ni atoms at sharp edges with the highest Ni potential. Calculations based on Density Functional Theory (DFT) were utilized to elucidate the reasons underlying the discovery. By examining the activation barrier for C-H bond breaking during the dissociative adsorption of CH_4, it was determined that the size and shape of the supported Ni nanoparticles, as well as the strength of the Ni support bonding and the charge transfer at the step edge, were critical for the high catalytic activity.

Table 1 summarizes the Dry Reforming Methane (DRM) utilizing CeO_2-based catalysts from 2015 to 2021.

Table 1. Summary of DRM with CeO_2-based catalysts from 2015 to 2021.

Active Metal	Preparation Method	Reaction Conditions	Conversion	Reference
Ni/CeO_2, $Ni\text{-}Co/CeO_2$, Co/CeO_2	Wetness impregnation method	700 °C	XCO_2 = 80% XCH_4 = 80% (Ni/CeO_2 and $Ni\text{-}Co/CeO_2$)	Ay et al. [82]
$Ni\text{-}Sn/Al_2O_3$ and $Ni\text{-}Sn/CeO_2\text{-}Al_2O_3$	Impregnation method	800 °C WHSV = 30,000 mlg^{-1} h^{-1}	XCO_2 = 85%	T. Stroud et al. [83]
Ni/CeO_2-SrO	Impregnation method	600 °C–800 °C	XCO_2 = 78% XCH_4 = 91% at 800 °C	Mallikarjun et al. [79]
$LaNi/MgAl_2O_4$ $CeNi/MgAl_2O_4$	Wet impregnation	600 °C–750 °C CH_4:CO_2 = 1:1 WHSV = 60,000 mlg^{-1} h^{-1}	XCO_2 = 96% XCH_4 = 92% (1.5Ce-Ni5)	Akiki et al. [84]
$0.42CeNi/Al_2O_3$HF ALD	Incipient wetness impregnation	850 °C	XCH_4 = 86.7% (1st cycle) XCH_4 = 88.4% (2nd cycle)	Jin et al. [85]
Ni-based Al_2O_3- CeO_2 supported monometallic Mo, bimetallic Fe-Mo and Pt-Mo, and trimetallic Pt-Fe-Mo	Incipient wetness impregnation	550–700 °C WHSV =12,000 mlg^{-1} h^{-1} Atmospheric pressure for 10 h	XCO_2 = 86% XCH_4 = 80% (co-doped Ni/ Al_2O_3-CeO_2 with Mo and Fe	Jawad et al. [68]
Ni-K/ CeO_2-Al_2O_3	Impregnation technique in two stages	650–800 °C	XCO_2 = 80.1% XCH_4 = 91.2%	Karemore et al. [86]
CeO_2 modification on Ni/Al_2O_3 catalyst and O_2 addition	Wetness incipient impregnation	600–800 °C	XCO_2 = 90% (800 °C) XCH_4 = 80% (800 °C)	Chein et al. [73]
HT Ce/Y0.2 HT Ce/Y0.4 HT Ce/Y0.6	Double-layered hydroxides modified with cerium (co-precipitation) and Yttrium (incipient wetness impregnation)	600–850 °C	Modification with the smallest loading of yttrium (0.2 wt%) led to highest CO_2 and CH_4 conversion XCO_2 = 97.4% (850 °C) XCH_4 = 96.2% (850 °C)	Swirk et al. [87]
4 wt% Ni/CeO_2 4 wt% $Ni/CeZrO_2$ (consisting of 20 wt% Zr)	Impregnation method	700 °C	$Ni/CeZrO_2$ is the better catalyst with conversion at 700 °C XCO_2 = 66% XCH_4 = 51%	Zhang F et al. [88]
Ni/Al_2O_3- CeO_2 and Ni/Al_2O_3-MgO	Impregnation and sol-gel methods	850 °C	H_2/CO ratio of 1 and H_2 yield of 94%	Hassani Rad SJ et al. [89]
Ni/Al_2O_3, Ni/Al_2O3- CeO_2, Ni/Al_2O3-La_2O_3	Sol gel method	800 °C	XCO_2 = 90% XCH_4 = 88%	Farooqi [72]
Yolk Shell catalysts. $Ni/ZnO@SiO_2$ vs. Ni/CeO_2 and Ni/Al_2O_3	Encapsulation of metal nanoparticles	850 °C	Conversion close to that equilibrium of CH_4. Reaching equilibrium for CO_2 conversion	Price et al. [90]
Sandwiched core-shell structured $Ni\text{-}SiO_2@CeO_2$	Nickel nanoparticles encapsulated between silica and ceria	600 °C GHSV= 200 L h^{-1} $gcat^{-1}$ CH_4:CO_2 = 3:2	CH_4 conversion activity = 0.12 mol CH_4 min^{-1} g $metal^{-1}$	Das et al. [91]
NiO-CeO_2 nanoparticles	Microemulsion	700 °C	XCO_2 = above 80% XCH_4 = above 80%	Cardenas et al. [93]
Ni-based mesoporous mixed CeO_2-Al_2O_3 oxide	One pot Evaporation Induced Self Assembly (EISA)	800 °C	XCO_2 = 85% XCH_4 = 80%	Marinho et al. [94]
Ni supported on metal doped ceria (Me-DC) catalyst $Ni/Me_{0.15}Ce_{0.85}O_{2-\varepsilon}$ With Me = Zr^{4+}, La^{3+} or Sm^{3+}	Citric acid synthetic route	800 °C	XCO_2 = 75% (5 h), 67% (50 h) XCH_4 = 53% (5 h), 49% (50 h) for Ni/CeO_2	Luisetto [65].
Nano-sized NiO-CeO_2 solid solution	Exsolution method	800 °C Feed gas composition: 50 vol% CH_4/50 vol% CO_2 5000 $Lkgcat^{-1}h^{-1}$	XCO_2 = 80% XCH_4 = 70%	Padi et al. [95]
Ni/CeO_2 catalyst	Photothermo DRM. Focalized UV-vis-IR irradiation using isotope labelling	450–700 °C	XCO_2 = 92.7% XCH_4 = 87.5%	Zhang, Q [96]
$Ni/CeO_2\text{-}SiO_2$-P (CeO_2 close contact with Ni NP) $Ni/CeO_2\text{-}SiO_2$-C (CeO_2 away from Ni NP)	Plasma decompose approach	700 °C	$Ni/CeO_2\text{-}SiO_2$-P XCO_2 = 87.3% XCH_4 = 78.5% $Ni/CeO_2\text{-}SiO_2$-C XCO_2 = 80.5% XCH_4 = 67.8%	X. Yan et al. [70]
$Ce_{0.5}Zr_{0.5}O_2$	Two step hydrothermal process	750 °C	XCO_2 = 80% XCH_4 = 88.4%	Tu, P.H [97]
Ni-MgO-CeO_2	Combined effects of titration rate during co-precipitation	800 °C	XCH_4 = 83.3%	Jeon et al. [101]

4. Summary of SRM with CeO_2-Based Catalysts from 2015 to 2021

Cifuentes et al. [103] discovered that 33% Si content in the support (RhPt/CeSi-33, Si:Ce ratio of 1:2) was the best for the catalyst as it decreased the basicity of the support, reduced the crystalline size of CeO_2, increased the catalyst surface area and decreased the active particle size. Moreover, it produced a maximum H_2 yield of 5.2+ 0.2 mol H_2/mol EtOH. The addition of Si reduced the relative basicity of CeO_2; hence, this composite

catalyst provides an equilibrium between the basicity (to maximize H_2 and excess of ethylene and coke formation) and acidity (to promote CH_4 formation and H_2O activation).

Iglesias I, et al. [104] compared nickel-based catalysts supported on pure or doped ceria (5% Zr, Pr, or La doping) produced through the co-precipitation urea technique in SRM reactions at 600, 750, and 900 °C and evaluated them under various feed conditions. At 600 °C, an increase in the vapor/methane ratio resulted in an increased hydrogen yield and decreased carbon creation and it was revealed that an intermediate calcination temperature (750 °C) maximized the nickel–support interaction, resulting in maximum methane conversion. OSC levels decrease in high-temperature and reductive environments. Zr stabilizes ceria, forming a ceria-zirconia solid solution in all composition ranges and improving textural features, thermal resistance, catalytic activity at lower temperatures and most importantly, oxygen storage/transport properties [105].

Zhang et al. [106] investigated the effect of doping different metals, namely Ti, Sn, Zr and Ce with Yttrium by the co-precipitation method to be used as supports for Ni-based catalysts in methane steam reforming. The structures of $Y_2Zr_2O_7$ and $Y_2Ce_2O_7$ compounds became defective fluorites and the surfaces of Ni/Y_2TiO_7 and Ni/Y_2CeO_7 had more abundant active oxygen species to suppress carbon formation. Ni/Y_2TiO_7 exhibited the highest activity, stability and coking resistance among the rest of the tested catalysts due to the largest amount of active surface oxygen species and the strongest Ni interaction with the support.

Iglesias I, et al. [107] optimized the nickel catalyst supported in zirconium-doped ceria in SRM at low temperatures and with a stoichiometric water/methane feed ratio. The formation of the zirconium tetragonal phase during synthesis was harmful to the reducibility of the solid and oxygen mobility, resulting in a better selectivity for low oxidation products. The effect of nickel loading on $Ce_{0.85}Zr_{0.15}O_{2-\delta}$ and pure ceria was evaluated, and it was determined that dispersion remained nearly constant up to 5%wt, was greater for the Zr-doped catalyst and decreased below 1% for the 10% catalyst. Figure 8 demonstrates that for each nickel loading, there were reduction events in the low temperature area (α and β) and the high temperature region (δ), demonstrating that the overall hydrogen consumption rose as the nickel loading increased. This study is consistent with Montini's comment on steam reforming, which indicated that the most investigated systems utilize ceria-zirconia mixed oxides due to their enhanced redox characteristics. The CeO_2-ZrO_2 oxides act as active supports for group 8, 9 and 10 metal nanoparticles, which serve as the catalytically active phases for hydrocarbon activation [108].

Lai et al. [109] developed approximately 6nm Ni-CeO_2-Al_2O_3 hybrid nano catalysts to achieve a low starting temperature (400 °C), high activity and high stability SRM by aerosol-based evaporation-induced self-assembly. This two-stage gas-phase method produced an ideal H_2 yield (~3x of the converted methane) and the amount of coke formation was reduced by >3x and had a high operation stability for 8 h. Fibril carbon, which has been identified as a non-deactivating carbon, was not found in the SEM images of Figure 9 (3 and 4) which proves that the addition of CeO_2 to the nanocomposite efficiently reduced carbon formation. The whisker carbon fibers were formed on the surface of the nanocomposite without the addition of CeO_2, as shown in the SEM images of Figure 9 (1 and 2).

Palma et al. [110] applied the Al_2O_3-CeO_2 catalysts to structured catalysts using washcoat slurries with loaded Ni which was prepared by wet impregnation for SRM. The methane conversion increased with the ceria content at the same temperature with XCH_4 = almost 100% selectivity to hydrogen. No coke formation was registered at temperatures higher than 700 °C due to the oxygen transfer capacity that promotes the gasification of carbon deposits.

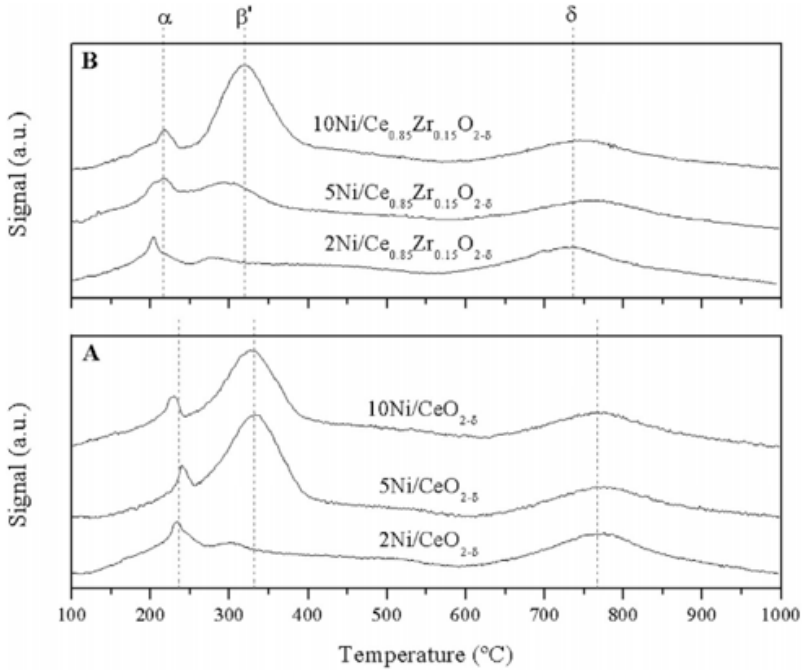

Figure 8. H_2-TPR profiles for yNi/CeO_2-δ (**A**) and yNi/$Ce_{0.85}Zr_{0.15}O_{2-\delta}$ (**B**) catalyst showedsimilar trendPeak α which attributed to highly reactive oxygen species lost relevance in contrast to Peak β which attributed to NiO and labile support oxygen concomitant reduction. The bulk oxygen reduction occurred on Peak δ in high temperature region. The 'α', 'β' and 'δ' mark the reduction process. Figure republished with permission from [107]. Copyright Elsevier, 2019.

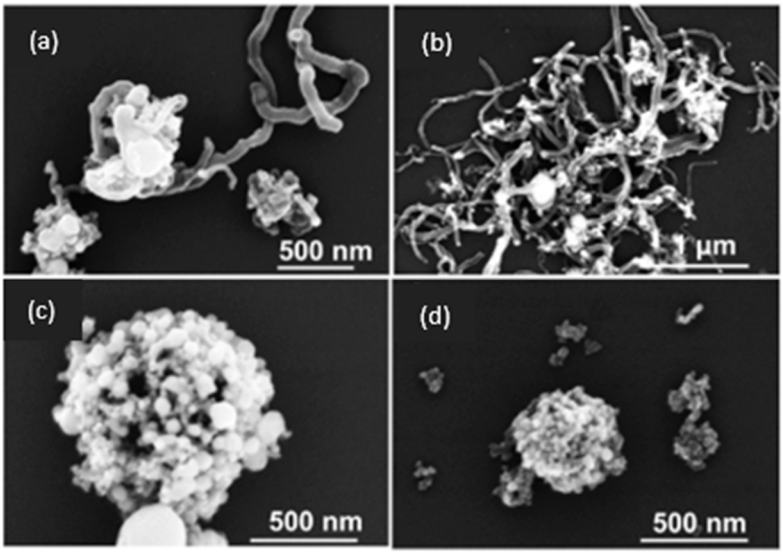

Figure 9. (**a**,**b**). SEM images shown whisker carbon fibers were deposited on the surface of 10Ni-0Ce-1Al and 10Ni-0Ce-5A1 (**c**,**d**). SEM images shown no fibril carbon on the surface of 10Ni-Ce-1Al and 10Ni-Ce-5Al. Figure republished with permission from ref [109]. Copyright ACS, 2019.

Torimoto et al. [111] investigated the support effects of CeO_2, Nb_2O_5 and Ta_2O_5 over Pd catalysts at low temperature SRM in an electric field to identify the factors controlling the activity of the catalyst support. All catalysts demonstrated activity at low temperatures exceeding the thermal equilibrium when tested in the electric field with the order of activity Pd/CeO_2 > Pd/Nb_2O_5 > Pd/Ta_2O_5 and the surface proton conduction was measured using electrochemical impedence spectroscopy (EIS) with the order of proton ability as CeO_2> Nb_2O_5 > Ta_2O_5. This work testified that as the adsorbed and activated amounts of

H_2O became larger, the proton conductivity became higher, then the catalyst was able to achieve high activity in the electric field for low temperature SRM.

Ghungrud SA et al. [112] developed multifunctional hybrid materials consisting of Ni, Co (in varying proportions 0–40%) and hydrotalcite using the co-precipitation method for sorption-enhanced SRM. Then, these materials were promoted with Ce species to improve the basicity for CO_2 adsorption and thermal stability and ultimately improved H_2 production. Ce-HM1 exhibited the maximum adsorption capacity, a better cyclic stability and a lower regeneration energy requirement.

Moogi et al. [113] compared the H_2 production and carbon formation of three types of Ni-based catalyst (Ni, Ni-La_2O_3 and Ni-La_2O_3-CeO_2) on mesoporous silica supports (SBA-15 and KIT-6) in glycerol steam reforming. It was highlighted during the N2-physisorption test that the addition of La_2O_3 increased the surface area of the catalyst by preventing pore mouth plugging in SBA-15. Ni-La_2O_3-CeO_2/SBA-15 gave the highest hydrogen concentrations of 62 mol% and less carbon formation on/near the nickel sites during the reforming reaction while the Ni-La_2O_3/SBA-15 catalyst experienced severe coke formation. The addition of CeO_2 to the catalyst increased the catalytic stability by facilitating the oxidative gasification of the carbon formed on the Ni active sites of catalyst during the reaction. The Ni-La_2O_3-CeO_2/KIT-6 formed a gaseous product with a lower H_2 concentration due to active methanation.

Liao et al. [114] investigated the catalytic activity of several supports in a microreactor for methanol steam reforming. The author demonstrated that a one-step hydrothermal method on the Al_2O_3 support produced CuO/ZnO/CeO_2/ZrO_2 nanoflowers with the maximum Ce^{3+}, oxygen vacancies and outstanding redox characteristics. At 310 °C, the nanoflowers catalyst on H-Al_2O_3 was composed of multiple nanosheets that grew aggressively on the ceramic surface, resulting in the highest loading strength of 99.8% methanol conversion and 0.16 mol/h H_2 production.

Salcedo et al. [115] used DFT to undertake a complete investigation of the SRM reaction on the surface of model Ni/CeO_2 (111) catalysts. The results indicated that low-loaded Ni/CeO_2 catalysts had distinct sites due to the metallic phases and the natures and interactions of the supports, which facilitate the easy activation of CH and OH bonds formed by CH_4 and H_2O, respectively. Therefore, the objective of improving the ceria-supported metal catalyst should be to modify it in such a way that the barrier to oxidation processes to create CO is reduced, which might be accomplished by employing Ni-based bimetallic catalysts. The results shed light on the molecular interactions between C and OH species during methane steam reforming on low-loaded Ni/CeO_2 catalysts, where metal support interactions are critical for binding and activating methane and water.

Wu et al. [116] demonstrated that adjusting the oxidation state of nickel using DFT simulations was efficient at regulating the activity and stability of partially oxidized Ni/CeO_2 (Ni-NiO/CeO_2) for the SRM reaction. This was accomplished by fine-tuning the metal/oxide ratio to ensure an optimal interaction with ceria. The predicted catalyst was validated experimentally, with NiO/CeO_2-364 °C demonstrating a higher performance for SMR, with methane conversion and H_2 production being stable throughout a 1500-min period at 700 °C.

Varkolu et al. [117] used the one-step evaporation-induced self-assembly (EISA) method to construct mesoporous Ni-CeO_2-ZrO_2-SiO_2 composite catalysts with high surface areas (approximately 200 m^2/g). The composite catalyst exhibited a strong interaction between the nickel and metal oxide supports, resulting in the creation of a CeO_2-ZrO_2 solid solution, which enhanced the catalyst's stability. The optimal catalyst, with a mole ratio of 1:2 CeO_2/ZrO_2 and a nickel loading of 20%, demonstrated constant catalytic activity for 30 h with a hydrogen yield of 75%. The optimal conditions for the reaction were a steam/carbon ratio of 2.5 and a temperature of 873 K.

Table 2 summarizes the Steam Reforming Methane (SRM) utilizing CeO_2-based catalysts from 2015 to 2021.

Table 2. Summary of SRM with CeO_2-based catalysts from 2015 to 2021.

Active Metal	Preparation Method	Reaction Conditions	Conversion/H_2 Yield	Reference
RhPt/CeSi-33	Co-impregnation Response Surface Methodology (RSM) determined the most appropriate metal loadings	400–700 °C GHSV = 65,200 h^{-1}	Ethanol conversion = 100%	Cifuentes et al. [103]
$Ni/Y_2Ti_2O_7$ $Ni/Y_2Sn_2O_7$ $Ni/Y_2Zr_2O_7$ Ni/Y_2CeO_7	Co-precipitation	600 °C	CH_4 conversion and H_2 yields of all catalyst follow the sequence $Ni/Y_2Ti_2O_7$ > Ni/Y_2CeO_7 ~ $Ni/Y_2Zr_2O_7$ > $Ni/Y_2Sn_2O_7$ XCH_4 = 85% for Ni/Y_2CeO_7 XCH_4 = 98% for $Ni/Y_2Ti_2O_7$	Zhang et al. [106]
$Ni/Ce_{1-x}Zr_xO_{2-\varepsilon}$	Co-precipitation method employing the homogenous thermal decomposition of urea	537–784 °C	XCH_4 = 70% H_2 yield = 65%	Iglesias, et al. [107]
Ni-CeO_2-Al_2O_3 hybrid nanoparticles clusters	(1) Gas phase evaporation-induced self-assembly (2) Two stage aerosol based thermal treatment	500–700 °C	Ideal H_2 yield (~3 times of the converted methane)	Lai et al. [109]
Al_2O_3-CeO_2 based washcoat slurries with loaded Ni	Wet impregnation	500–850 °C Atmospheric pressure WHSV = 15.8 mlg^{-1} h^{-1}	Methane conversion increased with the ceria content at the same temperature XCH_4 = almost 100% Selectivity to hydrogen	Palma et al. [110]
Pd/CeO_2 Pd/Nb_2O_5 Pd/Ta_2O_5	Impregnation method	200–500 °C SRM was conducted with and without electric field over Pd catalyst loaded with various oxides as support	The electric field promoted the activity drastically even at low temperature of 200 °C. Specific activity at 200 °C Pd/CeO_2 = 1 Pd/Nb_2O_5 = 0.66 Pd/Ta_2O_5 = 0.53	Torimoto et al. [111]
Promotion of Co-Ni/HTlc with Ce	Incipient wetness impregnation	450–600 °C	XCH_4 for: HM1 = 88.2% (550 °C) HM2 = 86.1% (550 °C) Ce-HM1 = 95.7% (500 °C) Ce-HM2 = 90.1% (500 °C)	Ghungrud SA et al. [112]
Ni/SBA-15 Ni-La_2O_3/SBA-15 Ni-La_2O_3-CeO_2/SBA-15 Ni-La_2O_3-CeO_2/KIT-6	incipient wetness impregnation	650 °C	Ni-La_2O_3-CeO_2/SBA-15 shown highest H_2 concentration of 62 mol% at LHSV of 5.8 h^{-1}	Moogi et al. [113]
CuO/ZnO/CeO_2/ZrO_2 nanoflowers catalyst on Al_2O_3 foam seramic	Hydrothermal	310 °C	99.8% methanol conversion rate 0.16 mol/h H_2 production.	Liao et al. [114]
Ni/CeO_2	Experiment of Ambient-Pressure XPS and DFT framework	26.85 °C–426.85 °C Low activation barrier (0.3–0.7 eV) for CH_4 dehydrogenation and H_2O activation	H_2 formation at low energy barrier	Salcedo et al. [115]
NiO/CeO_2-364 °C	DFT calculations	700 °C	XCH_4 = 96% H_2 production rate well maintained	Wu et al. [116]
Ni-CeO_2-ZrO_2-SiO_2 composite catalysts	One step EISA method using a block-copolymer	600 °C	n-butanol conversion = almost 100%	Varkolu et al. [117]

5. Conclusions

As the global energy transition accelerates, the creation of new and optimized DRM and SRM technologies is critical for long-term sustainability in the fight against climate change. A high carbon resistance, high-performance, long-lasting, and low-cost improved catalyst composition is critical to advance this agenda of commercializing reforming technology.

Over the last six years, researchers have concentrated on enhancing formulations for building CeO_2-based heterogeneous catalysts in DRM and SRM. Due to its extraordinary qualities, this rare earth has consistently functioned admirably as a heterogeneous catalyst, resulting in the production of a more desired product. The CeO_2-supported catalyst is stable

and the increase in stability has been attributed to an increase in the oxygen storage capacity, which enhances the CO_2 dissociative adsorption reaction and results in reduced carbon production. CeO_2 also performs admirably as a catalyst support, preventing the creation of carbon, which is reliant on the manner of catalyst preparation and the surface reactivity features caused by the substitution of Ce^{4+} with another cation. The optimal amount of CeO_2 loading was discovered to be between 5% and 10% for the optimal DRM performance. A high-quality catalyst should be capable of lowering the temperature necessary to initiate the reaction, hence reducing energy consumption and cost.

CeO_2 has been used more in DRM technologies than in SRM technologies over the last six years. Most researchers have focused on developing transition and rare earth metal catalysts with small particle sizes and a high sintering resistance. The encapsulation of metal nanoparticles, Evaporation Induced Self Assembly (EISA), Exsolution and Two-step hydrothermal methods are emerging new approaches for catalyst preparation that have significantly reduced the carbon deposition and have increased CH_4 and CO_2 conversion in DRM. The exsolution method could be extended to solid solutions containing reducible metal cations and to the creation of a variety of catalyst supports. The "one-pot" method of catalyst synthesis in a supercritical medium has also been discovered to be an effective method due to its ease of preparation and scalability. Theoretical calculations can provide direction in designing CeO_2-based catalysts through the control of the density and nature of the oxygen vacancies.

With so many features and advantages, it is easy to see why CeO_2 remains the most favored chemical element in catalyst formulation. Scientific advancements have shed new light on the relationship between metal–support interactions and carbon resistance in DRM and SRM. In the future, greater emphasis should be placed on the durability of the composite catalyst being created for immediate practicality and usefulness.

Author Contributions: Conceptualization, W.N.M.; writing—Original Draft preparation—W.N.M.; writing—Review and editing, W.N.M., W.N.R.W.I. and Z.Y. and funding acquisition, Z.Y. All authors have read and agreed to the published version of the manuscript.

Funding: This research was funded by Fundamental Research Grant Scheme, grant number FRGS/1/2019/TK02/UKM/01/2 from the Ministry of Higher Education, Malaysia.

Conflicts of Interest: The authors declare no conflict of interest

References

1. Noor, Z.; Yusuf, R.O.; Abba, A.H.; Abu Hassan, M.A.; Din, M.F.M. An overview for energy recovery from municipal solid wastes (MSW) in Malaysia scenario. *Renew. Sustain. Energy Rev.* **2013**, *20*, 378–384. [CrossRef]
2. Bian, Z.; Das, S.; Wai, M.H.; Hongmanorom, P.; Kawi, S. A Review on Bimetallic Nickel-Based Catalysts for CO_2 Reforming of Methane. *ChemPhysChem* **2017**, *18*, 3117–3134. [CrossRef] [PubMed]
3. United Nation. Adoption of the Paris agreement. In Proceedings of the Conference of the Parties, Paris, France, 30 November–12 December 2015.
4. Jang, W.-J.; Shim, J.-O.; Kim, H.-M.; Yoo, S.-Y.; Roh, H.-S. A review on dry reforming of methane in aspect of catalytic properties. *Catal. Today* **2018**, *324*, 15–26. [CrossRef]
5. Shell Global Shell Accelerates Drive for Net-Zero Emissions with Customer-First Strategy. Available online: https://www.shell.com/media/news-and-media-releases/2021/shell-accelerates-drive-for-net-zero-emissions-with-customer-first-strategy.html (accessed on 3 July 2021).
6. BP Sets Ambition for Net Zero by 2050, Fundamentally Changing Organisation to Deliver. Available online: https://www.bp.com/en/global/corporate/news-and-insights/press-releases/bernard-looney-announces-new-ambition-for-bp.html (accessed on 3 July 2021).
7. Petronas Declares Aspiration: To Achieve Net Zero Carbon Emissions by 2050. Available online: https://www.petronas.com/sustainability/net-zero-carbon-emissions (accessed on 3 July 2021).
8. Bhattacharjee, R.B. Climate Action Window Closing soon. *The Edge Malaysia*. 31 December 2020, pp. 62–63. Available online: https://www.theedgemarkets.com/article/climate-action-window-closing-soon (accessed on 31 December 2020).
9. Liu, Z.; Deng, Z.; Ciais, P.; Lei, R.; Davis, S.J.; Feng, S.; Zheng, B.; Cui, D.; Dou, X.; He, P.; et al. COVID-19 causes record decline in global CO_2 emissions. *arXiv* **2004**, arXiv:2004.13614.
10. Whitesides, M.; Crabtree, G. Don't Forget Long-Term Fundamental Research in Energy. *Science* **2007**, *315*, 796–798. [CrossRef]

11. Cai, X.; Hu, Y.H. Advances in catalytic conversion of methane and carbon dioxide to highly valuable products. *Energy Sci. Eng.* **2019**, *7*, 4–29. [CrossRef]
12. Olivier, J.G.J.; Peters, J.A.H.W. Trends in Global CO_2 and Total Greenhouse Gas Emissions: Report 2019. *PBL Neth. Environ. Assess. Agency* **2020**, *70*, 1–11.
13. Lewis, N.S.; Nocera, D.G. Powering the planet: Chemical challenges in solar energy utilization. *Proc. Natl. Acad. Sci. USA* **2006**, *103*, 15729–15735. [CrossRef]
14. Wigley, T.M.L.; Richels, R.G.; Edmonds, J.A. Economic and environmental choices in the stabilization of atmospheric CO_2 concentrations. *Nature* **1996**, *379*, 240–243. [CrossRef]
15. Steffen, W.; Hughes, L.; Pearce, A. *Climate Council Climate Change 2015: Growing Risks, Critical Choices*; Climate Council of Australia: Sydney, Australia, 2015; ISBN 978-099-430-107-9.
16. Sokolov, S.; Kondratenko, E.V.; Pohl, M.-M.; Barkschat, A.; Rodemerck, U. Stable low-temperature dry reforming of methane over mesoporous La2O3-ZrO_2 supported Ni catalyst. *Appl. Catal. B Environ.* **2011**, *113–114*, 19–30. [CrossRef]
17. Markewitz, P.; Kuckshinrichs, W.; Leitner, W.; Linssen, J.; Zapp, P.; Bongartz, R.; Schreiber, A.; Müller, T.E. Worldwide innovations in the development of carbon capture technologies and the utilization of CO_2. *Energy Environ. Sci.* **2012**, *5*, 7281–7305. [CrossRef]
18. Klankermayer, J.; Wesselbaum, S.; Beydoun, K.; Leitner, W. Selective Catalytic Synthesis Using the Combination of Carbon Dioxide and Hydrogen: Catalytic Chess at the Interface of Energy and Chemistry. *Angew. Chem. Int. Ed.* **2016**, *55*, 7296–7343. [CrossRef] [PubMed]
19. Ma, Y.; Gao, W.; Zhang, Z.; Zhang, S.; Tian, Z.; Liu, Y.; Ho, J.C.; Qu, Y. Regulating the surface of nanoceria and its applications in heterogeneous catalysis. *Surf. Sci. Rep.* **2018**, *73*, 1–36. [CrossRef]
20. Ampelli, C.; Perathoner, S.; Centi, G. CO_2 utilization: An enabling element to move to a resource- and energy-efficient chemical and fuel production. *Philos. Trans. R. Soc. Lond. Ser. A Math. Phys. Eng. Sci.* **2015**, *373*, 20140177. [CrossRef]
21. Pienkowski, L.; Motak, M.; Dabek, R.; Jaszczur, M. Use of HTGR Process Heat with Catalysts for Dry Reforming of Methane Using CO_2 to Singas for the Chemical Industry. 2018. Available online: https://www.semanticscholar.org/paper/Use-of-HTGR-process-heat-with-catalysts-for-dry-of-Motak-Dabek/b83f1ad63dff1a5e6aa0150a52b1b0a95e51784b (accessed on 23 August 2021).
22. Yusuf, M.; Farooqi, A.S.; Keong, L.K.; Hellgardt, K.; Abdullah, B. Latest Trends in Syngas Production Employing Compound Catalysts for Methane Dry Reforming. In *IOP Conference Series: Materials Science and Engineering*; IOP Publishing Ltd.: Bristol, UK, 2020; Volume 991.
23. Muraza, O.; Galadima, A. A review on coke management during dry reforming of methane. *Int. J. Energy Res.* **2015**, *39*, 1196–1216. [CrossRef]
24. Lavoie, J.-M. Review on dry reforming of methane, a potentially more environmentally-friendly approach to the increasing natural gas exploitation. *Front. Chem.* **2014**, *2*, 81. [CrossRef] [PubMed]
25. Asencios, Y.J.O.; Assaf, E.M. Combination of dry reforming and partial oxidation of methane on NiO-MgO-ZrO_2 catalyst: Effect of nickel content. *Fuel Process. Technol.* **2013**, *106*, 247–252. [CrossRef]
26. Van Beurden, P. On The Catalytic Aspects of Steam Reforming Methane—A Literature Survey. *ECN* **2004**, *3*, 1–27.
27. Meloni, E.; Martino, M.; Palma, V. A Short Review on Ni Based Catalysts and Related Engineering Issues for Methane Steam Reforming. *Catalysts* **2020**, *10*, 352. [CrossRef]
28. Kumar, N.; Shojaee, M.; Spivey, J.J. Catalytic bi-reforming of methane: From greenhouse gases to syngas. *Curr. Opin. Chem. Eng.* **2015**, *9*, 8–15. [CrossRef]
29. Niu, J.; Guo, F.; Ran, J.; Qi, W.; Yang, Z. Methane dry (CO_2) reforming to syngas (H_2/CO) in catalytic process: From experimental study and DFT calculations. *Int. J. Hydrogen Energy* **2020**, *45*, 30267–30287. [CrossRef]
30. Gao, J.; Hou, Z.; Lou, H.; Zheng, X. *Dry (CO_2) Reforming*, 1st ed.; Elsevier: Amsterdam, The Netherlands, 2011; ISBN 9780444535634.
31. Aramouni, N.A.K.; Touma, J.G.; Abu Tarboush, B.; Zeaiter, J.; Ahmad, M.N. Catalyst design for dry reforming of methane: Analysis review. *Renew. Sustain. Energy Rev.* **2018**, *82*, 2570–2585. [CrossRef]
32. Arora, S.; Prasad, R. An overview on dry reforming of methane: Strategies to reduce carbonaceous deactivation of catalysts. *RSC Adv.* **2016**, *6*, 108668–108688. [CrossRef]
33. Pakhare, D.; Spivey, J. A review of dry (CO_2) reforming of methane over noble metal catalysts. *Chem. Soc. Rev.* **2014**, *43*, 7813–7837. [CrossRef]
34. Jang, W.-J.; Jeong, D.-W.; Shim, J.-O.; Kim, H.-M.; Roh, H.-S.; Son, I.H.; Lee, S.J. Combined steam and carbon dioxide reforming of methane and side reactions: Thermodynamic equilibrium analysis and experimental application. *Appl. Energy* **2016**, *173*, 80–91. [CrossRef]
35. Zhu, J.; Peng, X.; Yao, L.; Deng, X.; Dong, H.; Tong, D.; Hu, C. Synthesis gas production from CO_2 reforming of methane over Ni-Ce/SiO_2 catalyst: The effect of calcination ambience. *Int. J. Hydrogen Energy* **2013**, *38*, 117–126. [CrossRef]
36. Daza, C.; Cabrera, C.; Moreno, S.; Molina, R. Syngas production from CO_2 reforming of methane using Ce-doped Ni-catalysts obtained from hydrotalcites by reconstruction method. *Appl. Catal. A Gen.* **2010**, *378*, 125–133. [CrossRef]
37. Santos, D.B.L.; Noronha, F.B.; Hori, C.E. Science Direct Bi-reforming of methane for hydrogen production using $LaNiO_3$/Ce x Zr_1-x O^2 as precursor material. *Int. J. Hydrogen Energy* **2020**, *45*, 13947–13959. [CrossRef]
38. Littlewood, P. *Low Temperature Dry Reforming of Methane with Nickel Manganese Oxide Catalysts*; Technische Universitaet Berlin: Berlin, Germany, 2015.
39. Fogler, H. *Essential of Chemical Reaction Engineering*; Pearson Education: London, UK, 2010; ISBN 978-013-714-612-3.

40. Ashcroft, A.T.; Cheetham, A.K.; Green, M.L.H.; Vernon, P.D.F. Partial oxidation of methane to synthesis gas using carbon dioxide. *Nature* **1991**, *352*, 225–226. [CrossRef]
41. Li, X.; Li, D.; Tian, H.; Zeng, L.; Zhao, Z.-J.; Gong, J. Dry reforming of methane over Ni/La_2O_3 nanorod catalysts with stabilized Ni nanoparticles. *Appl. Catal. B Environ.* **2017**, *202*, 683–694. [CrossRef]
42. Abdulrasheed, A.; Jalil, A.A.; Gambo, Y.; Ibrahim, M.; Hambali, H.U.; Hamid, M.Y.S. A review on catalyst development for dry reforming of methane to syngas: Recent advances. *Renew. Sustain. Energy Rev.* **2019**, *108*, 175–193. [CrossRef]
43. Abdullah, B.; Ghani, N.A.A.; Vo, D.-V.N. Recent advances in dry reforming of methane over Ni-based catalysts. *J. Clean. Prod.* **2017**, *162*, 170–185. [CrossRef]
44. Pawar, V.; Appari, S.; Monder, D.S.; Janardhanan, V.M. Study of the Combined Deactivation Due to Sulfur Poisoning and Carbon Deposition during Biogas Dry Reforming on Supported Ni Catalyst. *Ind. Eng. Chem. Res.* **2017**, *56*, 8448–8455. [CrossRef]
45. Védrine, J.C. Importance, features and uses of metal oxide catalysts in heterogeneous catalysis. *Chin. J. Catal.* **2019**, *40*, 1627–1636. [CrossRef]
46. Usman, M.; Wan Daud, W.M.A.; Abbas, H.F. Dry reforming of methane: Influence of process parameters—A review. *Renew. Sustain. Energy Rev.* **2015**, *45*, 710–744. [CrossRef]
47. Sun, Y.; Zhang, G.; Xu, Y.; Zhang, R. Catalytic performance of dioxide reforming of methane over Co/AC-N catalysts: Effect of nitrogen doping content and calcination temperature. *Int. J. Hydrogen Energy* **2019**, *44*, 16424–16435. [CrossRef]
48. Dębek, R.; Motak, M.; Grzybek, T.; Galvez, M.E.; Da Costa, P. A Short Review on the Catalytic Activity of Hydrotalcite-Derived Materials for Dry Reforming of Methane. *Catalysts* **2017**, *7*, 32. [CrossRef]
49. Liang, C.; Ma, Z.; Lin, H.; Ding, L.; Qiu, J.; Frandsen, W.; Su, D. Template preparation of nanoscale $CexFe_1-xO_2$ solid solutions and their catalytic properties for ethanol steam reforming. *J. Mater. Chem.* **2009**, *19*, 1417–1424. [CrossRef]
50. Kaneko, H.; Miura, T.; Ishihara, H.; Taku, S.; Yokoyama, T.; Nakajima, H.; Tamaura, Y. Reactive ceramics of CeO_2-MOx (M=Mn, Fe, Ni, Cu) for H_2 generation by two-step water splitting using concentrated solar thermal energy. *Energy* **2007**, *32*, 656–663. [CrossRef]
51. Chueh, W.C.; Haile, S.M. Ceria as a Thermochemical Reaction Medium for Selectively Generating Syngas or Methane from H_2O and CO_2. *ChemSusChem* **2009**, *2*, 735–739. [CrossRef]
52. Daza, C.E.; Moreno, S.; Molina, R. Ce-incorporation in mixed oxides obtained by the self-combustion method for the preparation of high performance catalysts for the CO_2 reforming of methane. *Catal. Commun.* **2010**, *12*, 173–179. [CrossRef]
53. Younis, A.; Chu, D.; Li, S. Cerium Oxide Nanostructures and their Applications. *Funct. Nanomater.* **2016**, *3*, 53–68. [CrossRef]
54. Malavasi, L.; Fisher, C.A.J.; Islam, M.S. Oxide-ion and proton conducting electrolyte materials for clean energy applications: Structural and mechanistic features. *Chem. Soc. Rev.* **2010**, *39*, 4370–4387. [CrossRef] [PubMed]
55. Rodriguez, J.A.; Grinter, D.C.; Liu, Z.; Palomino, R.M.; Senanayake, S.D. Ceria-based model catalysts: Fundamental studies on the importance of the metal-ceria interface in CO oxidation, the water–gas shift, CO_2 hydrogenation, and methane and alcohol reforming. *Chem. Soc. Rev.* **2017**, *46*, 1824–1841. [CrossRef]
56. Trovarelli, A. Catalytic Properties of Ceria and CeO_2-Containing Materials. *Catal. Rev.* **1996**, *38*, 439–520. [CrossRef]
57. Chen, W.; Zhao, G.; Xue, Q.; Chen, L.; Lu, Y. High carbon-resistance Ni/$CeAlO_3$-Al_2O_3 catalyst for CH_4/CO_2 reforming. *Appl. Catal. B Environ.* **2013**, *136-137*, 260–268. [CrossRef]
58. Aneggi, E.; de Leitenburg, C.; Boaro, M.; Fornasiero, P.; Trovarelli, A. *Catalytic Applications of Cerium Dioxide*; Elsevier: Amsterdam, The Netherlands, 2020; ISBN 978-012-815-661-2.
59. Shan, Y.; Liu, Y.; Li, Y.; Yang, W. A review on application of cerium-based oxides in gaseous pollutant purification. *Sep. Purif. Technol.* **2020**, *250*, 117181. [CrossRef]
60. Dos Santos, R.G.; Alencar, A.C. Biomass-derived syngas production via gasification process and its catalytic conversion into fuels by Fischer Tropsch synthesis: A review. *Int. J. Hydrogen Energy* **2020**, *45*, 18114–18132. [CrossRef]
61. Wang, X.; Shi, A.; Duan, Y.; Wang, J.; Shen, M. Catalytic performance and hydrothermal durability of CeO_2–V_2O_5–ZrO_2/WO_3–TiO_2 based NH_3-SCR catalysts. *Catal. Sci. Technol.* **2012**, *2*, 1386–1395. [CrossRef]
62. Mullins, D.R. The surface chemistry of cerium oxide. *Surf. Sci. Rep.* **2015**, *70*, 42–85. [CrossRef]
63. Kim, M.-J.; Youn, J.-R.; Kim, H.J.; Seo, M.W.; Lee, D.; Go, K.S.; Lee, K.B.; Jeon, S.G. Effect of surface properties controlled by Ce addition on CO_2 methanation over Ni/Ce/Al_2O_3 catalyst. *Int. J. Hydrogen Energy* **2020**, *45*, 24595–24603. [CrossRef]
64. Di Monte, R.; Kašpar, J. Heterogeneous environmental catalysis—A gentle art: CeO_2-ZrO_2 mixed oxides as a case history. *Catal. Today* **2005**, *100*, 27–35. [CrossRef]
65. Luisetto, I.; Tuti, S.; Romano, C.; Boaro, M.; Di Bartolomeo, E.; Kesavan, J.K.; Kumar, S.S.; Selvakumar, K. Dry reforming of methane over Ni supported on doped CeO_2: New insight on the role of dopants for CO_2 activation. *J. CO_2 Util.* **2019**, *30*, 63–78. [CrossRef]
66. Benrabaa, R.; Löfberg, A.; Caballero, J.G.; Bordes-Richard, E.; Rubbens, A.; Vannier, R.-N.; Boukhlouf, H.; Barama, A. Sol-gel synthesis and characterization of silica supported nickel ferrite catalysts for dry reforming of methane. *Catal. Commun.* **2015**, *58*, 127–131. [CrossRef]
67. Amjad, U.-E.; Quintero, C.W.M.; Ercolino, G.; Italiano, C.; Vita, A.; Specchia, S. Methane Steam Reforming on the Pt/CeO_2 Catalyst: Effect of Daily Start-Up and Shut-Down on Long-Term Stability of the Catalyst. *Ind. Eng. Chem. Res.* **2019**, *58*, 16395–16406. [CrossRef]

68. Jawad, A.; Rezaei, F.; Rownaghi, A.A. Highly efficient Pt/Mo-Fe/Ni-based Al_2O_3-CeO_2 catalysts for dry reforming of methane. *Catal. Today* **2019**, *350*, 80–90. [CrossRef]
69. Vita, A.; Pino, L.; Cipitì, F.; Laganà, M.; Recupero, V. Biogas as renewable raw material for syngas production by tri-reforming process over $NiCeO_2$ catalysts: Optimal operative condition and effect of nickel content. *Fuel Process. Technol.* **2014**, *127*, 47–58. [CrossRef]
70. Yan, X.; Hu, T.; Liu, P.; Li, S.; Zhao, B.; Zhang, Q.; Jiao, W.; Chen, S.; Wang, P.; Lu, J.; et al. Highly efficient and stable Ni/CeO_2-SiO_2 catalyst for dry reforming of methane: Effect of interfacial structure of Ni/CeO_2 on SiO_2. *Appl. Catal. B Environ.* **2019**, *246*, 221–231. [CrossRef]
71. Pérez, L.P.; Sepúlveda-Escribano, A. Low temperature glycerol steam reforming on bimetallic PtSn/C catalysts: On the effect of the Sn content. *Fuel* **2017**, *194*, 222–228. [CrossRef]
72. Farooqi, A.S.; Al-Swai, B.M.; Ruslan, F.H.B.; Zabidi, N.A.M.; Saidur, R.; Muhammad, S.A.F.S.; Abdullah, B. Syngas production via dry reforming of methane over Nibased catalysts. *IOP Conf. Ser. Mater. Sci. Eng.* **2020**, *736*, 042007. [CrossRef]
73. Chein, R.-Y.; Fung, W.-Y. Syngas production via dry reforming of methane over CeO_2 modified Ni/Al_2O_3 catalysts. *Int. J. Hydrogen Energy* **2019**, *44*, 14303–14315. [CrossRef]
74. Huang, J.; Ma, R.; Gao, Z.; Shen, C.; Huang, W. Characterization and Catalytic Activity of CeO_2-Ni/Mo/SBA-15 Catalysts for Carbon Dioxide Reforming of Methane. *Chin. J. Catal.* **2012**, *33*, 637–644. [CrossRef]
75. Du, X.; Zhang, D.; Shi, L.; Gao, R.; Zhang, J. Morphology Dependence of Catalytic Properties of Ni/CeO_2 Nanostructures for Carbon Dioxide Reforming of Methane. *J. Phys. Chem. C* **2012**, *116*, 10009–10016. [CrossRef]
76. Li, S.; Xu, Y.; Chen, Y.; Li, W.; Lin, L.; Li, M.; Deng, Y.; Wang, X.; Ge, B.; Yang, C.; et al. Tuning the Selectivity of Catalytic Carbon Dioxide Hydrogenation over Iridium/Cerium Oxide Catalysts with a Strong Metal-Support Interaction. *Angew. Chem.* **2017**, *129*, 10901–10905. [CrossRef]
77. Li, D.; Zeng, L.; Li, X.; Wang, X.; Ma, H.; Assabumrungrat, S.; Gong, J. Ceria-promoted Ni/SBA-15 catalysts for ethanol steam reforming with enhanced activity and resistance to deactivation. *Appl. Catal. B Environ.* **2015**, *176-177*, 532–541. [CrossRef]
78. Jiang, X.; Nie, X.; Guo, X.; Song, C.; Chen, J.G. Recent Advances in Carbon Dioxide Hydrogenation to Methanol via Heterogeneous Catalysis. *Chem. Rev.* **2020**, *120*, 7984–8034. [CrossRef] [PubMed]
79. Mallikarjun, G.; Sagar, T.; Swapna, S.; Raju, N.; Chandrashekar, P.; Lingaiah, N. Hydrogen rich syngas production by bi-reforming of methane with CO_2 over Ni supported on CeO_2-SrO mixed oxide catalysts. *Catal. Today* **2020**, *356*, 597–603. [CrossRef]
80. Paksoy, A.I.; Caglayan, B.S.; Ozensoy, E.; Ökte, A.; Aksoylu, A.E. The effects of Co/Ce loading ratio and reaction conditions on CDRM performance of Co Ce/ZrO_2 catalysts. *Int. J. Hydrogen Energy* **2018**, *43*, 4321–4334. [CrossRef]
81. Sun, Y.; Zhang, G.; Xu, Y.; Zhang, R. Dry reforming of methane over Co-Ce-M/AC-N catalyst: Effect of promoters (Ca and Mg) and preparation method on catalytic activity and stability. *Int. J. Hydrogen Energy* **2019**, *44*, 22972–22982. [CrossRef]
82. Ay, H.; Üner, D. Dry reforming of methane over CeO_2 supported Ni, Co and Ni–Co catalysts. *Appl. Catal. B Environ.* **2015**, *179*, 128–138. [CrossRef]
83. Stroud, T.; Smith, T.; le Saché, E.; Santos, J.L.; Centeno, M.A.; Arellano-Garcia, H.; Odriozola, J.A.; Reina, T. Chemical CO_2 recycling via dry and bi reforming of methane using Ni-Sn/Al_2O_3 and Ni-Sn/CeO_2-Al_2O_3 catalysts. *Appl. Catal. B Environ.* **2017**, *224*, 125–135. [CrossRef]
84. Akiki, E.; Akiki, D.; Italiano, C.; Vita, A.; Abbas-Ghaleb, R.; Chlala, D.; Ferrante, G.D.; Laganà, M.; Pino, L.; Specchia, S. Production of hydrogen by methane dry reforming: A study on the effect of cerium and lanthanum on Ni/$MgAl_2O_4$ catalyst performance. *Int. J. Hydrogen Energy* **2020**, *45*, 21392–21408. [CrossRef]
85. Jin, B.; Shang, Z.; Li, S.; Jiang, Y.-B.; Gu, X.; Liang, X. Reforming of methane with carbon dioxide over cerium oxide promoted nickel nanoparticles deposited on 4-channel hollow fibers by atomic layer deposition. *Catal. Sci. Technol.* **2020**, *10*, 3212–3222. [CrossRef]
86. Karemore, A.L.; Sinha, R.; Chugh, P.; Vaidya, P.D. Mixed reforming of methane over Ni–K/CeO_2–Al_2O_3: Study of catalyst performance and reaction kinetics. *Int. J. Hydrogen Energy* **2020**, *46*, 5223–5233. [CrossRef]
87. Świrk, K.; Rønning, M.; Motak, M.; Beaunier, P.; Da Costa, P.; Grzybek, T. Ce- and Y-Modified Double-Layered Hydroxides as Catalysts for Dry Reforming of Methane: On the Effect of Yttrium Promotion. *Catalysts* **2019**, *9*, 56. [CrossRef]
88. Zhang, F.; Liu, Z.; Chen, X.; Rui, N.; Betancourt, L.E.; Lin, L.; Xu, W.; Sun, C.-J.; Abeykoon, A.M.M.; Rodriguez, J.A.; et al. Effects of Zr Doping into Ceria for the Dry Reforming of Methane over Ni/$CeZrO_2$ Catalysts: In Situ Studies with XRD, XAFS, and AP-XPS. *ACS Catal.* **2020**, *10*, 3274–3284. [CrossRef]
89. Rad, S.J.H.; Haghighi, M.; Eslami, A.A.; Rahmani, F.; Rahemi, N. Sol-gel vs. impregnation preparation of MgO and CeO_2 doped Ni/Al_2O_3 nanocatalysts used in dry reforming of methane: Effect of process conditions, synthesis method and support composition. *Int. J. Hydrogen Energy* **2016**, *41*, 5335–5350. [CrossRef]
90. Price, C.A.H.; Earles, E.; Pastor-Pérez, L.; Liu, J.; Reina, T.R. Advantages of Yolk Shell Catalysts for the DRM: A Comparison of Ni/ZnO@SiO_2 vs. Ni/CeO_2 and Ni/Al_2O_3. *Chemistry* **2018**, *1*, 3–16. [CrossRef]
91. Das, S.; Ashok, J.; Bian, Z.; Dewangan, N.; Wai, M.; Du, Y.; Borgna, A.; Hidajat, K.; Kawi, S. Silica-Ceria sandwiched Ni core-shell catalyst for low temperature dry reforming of biogas: Coke resistance and mechanistic insights. *Appl. Catal. B Environ.* **2018**, *230*, 220–236. [CrossRef]
92. Han, K.; Yu, W.; Xu, L.; Deng, Z.; Yu, H.; Wang, F. Reducing carbon deposition and enhancing reaction stability by ceria for methane dry reforming over Ni@SiO_2@CeO_2 catalyst. *Fuel* **2021**, *291*, 120182. [CrossRef]

93. Cárdenas-Arenas, A.; Bailón-García, E.; Lozano-Castelló, D.; Da Costa, P.; Bueno-López, A. Stable NiO-CeO_2 nanoparticles with improved carbon resistance for methane dry reforming. *J. Rare Earths* **2020**, *40*, 57–62. [CrossRef]
94. Marinho, A.L.; Toniolo, F.S.; Noronha, F.B.; Epron, F.; Duprez, D.; Bion, N. Highly active and stable Ni dispersed on mesoporous CeO_2-Al_2O_3 catalysts for production of syngas by dry reforming of methane. *Appl. Catal. B Environ.* **2020**, *281*, 119459. [CrossRef]
95. Padi, S.P.; Shelly, L.; Komarala, E.P.; Schweke, D.; Hayun, S.; Rosen, B.A. Coke-free methane dry reforming over nano-sized NiO-CeO_2 solid solution after exsolution. *Catal. Commun.* **2020**, *138*, 105951. [CrossRef]
96. Zhang, Q.; Mao, M.; Li, Y.; Yang, Y.; Huang, H.; Jiang, Z.; Hu, Q.; Wu, S.; Zhao, X. Novel photoactivation promoted light-driven CO_2 reduction by CH_4 on Ni/CeO_2 nanocomposite with high light-to-fuel efficiency and enhanced stability. *Appl. Catal. B Environ.* **2018**, *239*, 555–564. [CrossRef]
97. Tu, P.; Sakamoto, M.; Sasaki, K.; Shiratori, Y. Synthesis of flowerlike ceria–zirconia solid solution for promoting dry reforming of methane. *Int. J. Hydrogen Energy* **2021**. [CrossRef]
98. Simonov, M.; Bespalko, Y.; Smal, E.; Valeev, K.; Fedorova, V.; Krieger, T.; Sadykov, V. Nickel-Containing Ceria-Zirconia Doped with Ti and Nb. Effect of Support Composition and Preparation Method on Catalytic Activity in Methane Dry Reforming. *Nanomaterials* **2020**, *10*, 1281. [CrossRef]
99. Fedorova, V.; Simonov, M.; Valeev, K.; Bespalko, Y.; Smal, E.; Eremeev, N.; Sadovskaya, E.; Krieger, T.; Ishchenko, A.; Sadykov, V. Kinetic Regularities of Methane Dry Reforming Reaction on Nickel-Containing Modified Ceria-Zirconia. *Energies* **2021**, *14*, 2973. [CrossRef]
100. Li, B.; Yuan, X.; Li, B.; Wang, X. Ceria-modified nickel supported on porous silica as highly active and stable catalyst for dry reforming of methane. *Fuel* **2021**, *301*, 121027. [CrossRef]
101. Jeon, K.-W.; Kim, H.-M.; Kim, B.-J.; Lee, Y.-L.; Na, H.-S.; Shim, J.-O.; Jang, W.-J.; Roh, H.-S. Synthesis gas production from carbon dioxide reforming of methane over Ni-MgO catalyst: Combined effects of titration rate during co-precipitation and CeO_2 addition. *Fuel Process. Technol.* **2021**, *219*, 106877. [CrossRef]
102. Lustemberg, P.G.; Mao, Z.; Salcedo, A.; Irigoyen, B.; Ganduglia-Pirovano, M.V.; Campbell, C.T. Nature of the Active Sites on Ni/CeO_2 Catalysts for Methane Conversions. *ACS Catal.* **2021**, *11*, 10604–10613. [CrossRef]
103. Cifuentes, B.; Hernández, M.; Monsalve, S.; Cobo, M. Hydrogen production by steam reforming of ethanol on a RhPt/CeO_2/SiO_2 catalyst: Synergistic effect of the Si:Ce ratio on the catalyst performance. *Appl. Catal. A Gen.* **2016**, *523*, 283–293. [CrossRef]
104. Iglesias, I.; Baronetti, G.; Mariño, F. Ni/$Ce_{0.95}M_{0.05}O_2$−d (M = Zr, Pr, La) for methane steam reforming at mild conditions. *Int. J. Hydrogen Energy* **2017**, *42*, 29735–29744. [CrossRef]
105. Kambolis, A.; Matralis, H.; Trovarelli, A.; Papadopoulou, C. Ni/CeO_2-ZrO_2 catalysts for the dry reforming of methane. *Appl. Catal. A Gen.* **2010**, *377*, 16–26. [CrossRef]
106. Zhang, X.; Peng, L.; Fang, X.; Cheng, Q.; Liu, W.; Peng, H.; Gao, Z.; Zhou, W.; Wang, X. Ni/$Y_2B_2O_7$ (B Ti, Sn, Zr and Ce) catalysts for methane steam reforming: On the effects of B site replacement. *Int. J. Hydrogen Energy* **2018**, *43*, 8298–8312. [CrossRef]
107. Iglesias, I.; Baronetti, G.; Alemany, L.J.; Mariño, F. Insight into Ni/Ce_1-xZrxO_2-δ support interplay for enhanced methane steam reforming. *Int. J. Hydrogen Energy* **2019**, *44*, 3668–3680. [CrossRef]
108. Montini, T.; Melchionna, M.; Monai, M.; Fornasiero, P. Fundamentals and Catalytic Applications of CeO_2-Based Materials. *Chem. Rev.* **2016**, *116*, 5987–6041. [CrossRef]
109. Lai, G.-H.; Lak, J.H.; Tsai, D.-H. Hydrogen Production via Low-Temperature Steam-Methane Reforming Using Ni-CeO_2-Al_2O_3 Hybrid Nanoparticle Clusters as Catalysts. *ACS Appl. Energy Mater.* **2019**, *2*, 7963–7971. [CrossRef]
110. Palma, V.; Meloni, E.; Renda, S.; Martino, M. Catalysts for Methane Steam Reforming Reaction: Evaluation of CeO_2 Addition to Alumina-Based Washcoat Slurry Formulation. *C-J. Carbon Res.* **2020**, *6*, 52. [CrossRef]
111. Torimoto, M.; Ogo, S.; Hisai, Y.; Nakano, N.; Takahashi, A.; Ma, Q.; Gil Seo, J.; Tsuneki, H.; Norby, T.; Sekine, Y. Support effects on catalysis of low temperature methane steam reforming. *RSC Adv.* **2020**, *10*, 26418–26424. [CrossRef]
112. Ghungrud, S.A.; Dewoolkar, K.D.; Vaidya, P.D. Cerium-promoted bi-functional hybrid materials made of Ni, Co and hydrotalcite for sorption-enhanced steam methane reforming (SESMR). *Int. J. Hydrogen Energy* **2018**, *44*, 694–706. [CrossRef]
113. Moogi, S.; Lee, I.-G.; Hwang, K.-R. Catalytic steam reforming of glycerol over Ni-La_2O_3-CeO_2/SBA-15 catalyst for stable hydrogen-rich gas production. *Int. J. Hydrogen Energy* **2020**, *45*, 28462–28475. [CrossRef]
114. Liao, M.; Guo, C.; Guo, W.; Hu, T.; Xie, J.; Gao, P.; Xiao, H. One-step growth of CuO/ZnO/CeO_2/ZrO_2 nanoflowers catalyst by hydrothermal method on Al_2O_3 support for methanol steam reforming in a microreactor. *Int. J. Hydrogen Energy* **2021**, *46*, 9280–9291. [CrossRef]
115. Salcedo, A.; Lustemberg, P.G.; Rui, N.; Palomino, R.M.; Liu, Z.; Nemsak, S.; Senanayake, S.D.; Rodriguez, J.A.; Ganduglia-Pirovano, M.V.; Irigoyen, B. Reaction Pathway for Coke-Free Methane Steam Reforming on a Ni/CeO_2 Catalyst: Active Sites and the Role of Metal-Support Interactions. *ACS Catal.* **2021**, *11*, 8327–8337. [CrossRef] [PubMed]
116. Wu, C.; Xiao, Z.; Wang, L.; Li, G.; Zhang, X.; Wang, L. Modulating oxidation state of Ni/CeO_2 catalyst for steam methane reforming: A theoretical prediction with experimental verification. *Catal. Sci. Technol.* **2021**, *11*, 1965–1973. [CrossRef]
117. Varkolu, M.; Kunamalla, A.; Jinnala, S.A.K.; Kumar, P.; Maity, S.K.; Shee, D. Role of CeO_2/ZrO_2 mole ratio and nickel loading for steam reforming of n-butanol using Ni-CeO_2-ZrO_2-SiO_2 composite catalysts: A reaction mechanism. *Int. J. Hydrogen Energy* **2020**, *46*, 7320–7335. [CrossRef]